



HAL
open science

Browsing and non-browsing extant and extinct giraffids Evidence from dental microwear textural analysis

Gildas Merceron, Marc Colyn, Denis Geraads

► **To cite this version:**

Gildas Merceron, Marc Colyn, Denis Geraads. Browsing and non-browsing extant and extinct giraffids Evidence from dental microwear textural analysis. *Palaeogeography, Palaeoclimatology, Palaeoecology*, 2018, 505, pp.128-139. 10.1016/j.palaeo.2018.05.036 . hal-01834854v2

HAL Id: hal-01834854

<https://univ-rennes.hal.science/hal-01834854v2>

Submitted on 6 Sep 2018

HAL is a multi-disciplinary open access archive for the deposit and dissemination of scientific research documents, whether they are published or not. The documents may come from teaching and research institutions in France or abroad, or from public or private research centers.

L'archive ouverte pluridisciplinaire **HAL**, est destinée au dépôt et à la diffusion de documents scientifiques de niveau recherche, publiés ou non, émanant des établissements d'enseignement et de recherche français ou étrangers, des laboratoires publics ou privés.

1 Browsing and non-browsing extant and extinct giraffids: evidence from dental microwear
2 textural analysis.

3

4 Gildas MERCERON¹, Marc COLYN², Denis GERAADS³

5

6 ¹ Palevoprim (UMR 7262, CNRS & Université de Poitiers, France)

7 ² ECOBIO (UMR 6553, CNRS & Université de Rennes 1, Station Biologique de Paimpont,
8 France)

9 ³ CR2P (UMR 7207, Sorbonne Universités, MNHN, CNRS, UPMC, France)

10

11 ¹Corresponding author: gildas.merceron@univ-poitiers.fr

12

13 Abstract:

14

15 Today, the family Giraffidae is restricted to two genera endemic to the African
16 continent, *Okapia* and *Giraffa*, but, with over ten genera and dozens of species, it was far
17 more diverse in the Old World during the late Miocene. We attempt to describe here how
18 several species may have shared feeding resources in the Eastern Mediterranean. Dietary
19 preferences were explored by means of Dental Microwear Textural Analysis in combination
20 with estimation of body mass and the maximum height at which the various species were able
21 to browse.

22 One of our main results concerns the modern okapi, *Okapia johnstoni*. It is a forest
23 dweller usually regarded as a browser, but we show that it might also forage on tough plants,
24 possibly herbaceous monocots. Such feeding habits including portions of herbaceous
25 monocotyledons were also found for some extinct species, especially the genera *Samotherium*
26 and *Palaeotragus*. *Palaeogiraffa* shows a contrasted pattern: the specimens of *P. pamiri* from
27 a site in Thrace were leaf-dominant browsers whereas those belonging to *P. major* and *P.*
28 *macedoniae* from the Axios valley in Greece ingested herbaceous monocotyledons.
29 *Helladotherium duvernoyi*, the only sivatheriine analyzed here is described as a leaf-dominant
30 browser. The giraffine *Bohlinia attica* also falls within the leaf-dominant browser category
31 but could browse on higher foliages than *H. duvernoyi*. On the whole, the reconstructed diets
32 confirm the relationship between more grazing habits and smaller premolars, but not with
33 higher dental crown height.

34

35 Keywords: Tooth, Ruminant, Neogene, Diet, Ecology

36

37 **1. Introduction**

38 Today, giraffids are poorly diverse with only two genera, *Okapia* and *Giraffa* (Agaba
39 et al., 2016), both endemic to the African continent. The okapi *Okapia johnstoni* is endemic to
40 the north east of the Democratic Republic of Congo in the Congo Basin. There, the okapi is
41 confined to dense equatorial forest, which explains why its anatomical description in a
42 scientific journal dates back only to the early 20th century. *Okapia johnstoni* is unknown as a
43 fossil, but its discovery has generated several hypotheses regarding its relationships with the
44 giraffe and the many species of extinct giraffids (Colbert, 1938; Thenius, 1992). The modern
45 giraffe has a wide range of distribution in subsaharan Africa. The genus dates back to the
46 early Pliocene. A large part of the evolutionary history of the Giraffidae did not take place in
47 Africa but in Eurasia during the Neogene (Solounias et al., 2010). With over 10 genera and
48 dozens of named species that can be conveniently grouped in three subfamilies (Sivatheriinae,
49 Giraffinae, Palaeotraginae), the family reached its highest diversity during the late Miocene.
50 They share with modern taxa a small set of synapomorphies such as large body size, bilobate
51 canine, and a molariform fourth premolar, but their skin-covered cranial appendages are not
52 exclusive to the family (Geraads, 1986). A phylogenetic analysis of giraffids based upon new
53 material from the late Miocene of Spain confirmed the monophylies of the two subfamilies
54 Sivatheriinae and Giraffinae. However, the Sivatheriinae appear as the sister-group of the
55 genus *Samotherium* and are thus rooted within the Palaeotraginae, whose paraphyletic status
56 is thus emphasized (Ríos et al., 2017, 2016).

57 The present study aims at determining the feeding ecology of the extinct giraffids from
58 the late Miocene of Eastern Mediterranean in regard to their differences in morphology
59 mirroring the phylogeny. We use dental microwear textural analysis (DMTA, hereafter) to
60 specify the dietary habits. First, we discuss the relations between dietary habits and dental
61 microwear textural parameters on extant species of ruminants. This allows us to interpret and

62 discuss the dental microwear textural parameters of species with unknown feeding habits.
63 Before applying these parameters to extinct species of giraffids to identify their feeding type,
64 we question the dietary habits of the present-day okapi, a species assumed to be a browser on
65 the basis of a single field ecological survey (Hart and Hart, 1989). Second, we discuss the
66 dietary reconstruction of these extinct species in relation to the morphology, and notably the
67 body mass estimates and the length of the metacarpal bone, the latter feature being a proxy to
68 assess the maximum height at which a given species can access the food resources. We may
69 expect that smaller species with shorter forelimbs are more prone to include herbaceous
70 vegetation than large species of giraffids. This permits us to evaluate the ecological niche
71 partitioning when species co-occurred in the fossil record, suggesting an overlap of their
72 home-range, such as at Pikermi (Greece) and Hadjidimovo (Bulgaria). Besides, considering
73 that none of these giraffids displayed post canine hypsodont cheekteeth, we may expect that
74 none of these giraffids included herbaceous vegetation in its diet. However, an early pioneer
75 study on dental abrasion (Solounias et al., 1988) challenged the hypothesis of browsing habits
76 among all extinct giraffids. These authors depicted *Samotherium boissieri*, a late Miocene
77 giraffid from Samos Island (Greece) as a mixed feeding species incorporating silica-bearing
78 herbaceous monocotyledons in its diet. Previous dental wear analysis on material from
79 historical collections of Samos and Pikermi also found out differences between giraffids
80 species (Danowitz et al., 2016; Solounias, 1988; Solounias et al., 2000). We here go further in
81 significantly increasing the sample with new material from northern Greece, Bulgaria and
82 Turkey.

83

84 **2. Material and Methods**

85 *2.1. Material*

86 The dental microwear textures of extinct giraffids are compared with those of present-
87 day species of ruminants with known differences in diet (housed in the following museum and
88 institutions: AMNHS Aegean Museum of Natural History of Samos, Greece; NHMEU Natural
89 History Museum of the Ege University of Izmir, Turkey; NHML Natural History Museum of
90 London, UK; NHMB Naturhistorisches Museum Basel, Switzerland; SMNS Staatliches
91 Museum für Naturkunde Stuttgart, Germany; SMNK Staatliches Museum für Naturkunde
92 Karlsruhe, Germany; SNG Senckenberg Museum, Frankfurt, Germany; UP Paleovoprim lab,
93 University of Poitiers, France; KNM National Museums of Kenya, Nairobi, Kenya; MNHN
94 Muséum National d'Histoire Naturelle, Paris, France; MRAC Central African Royal Museum
95 of Tervuren, Belgium; FSL Collection de Géologie de la Faculté des Sciences de l'Université
96 de Lyon, France; AM-NHNMS Assenovgrad Museum; a division of the National Museum of
97 Natural History of Sofia, Bulgaria). Instead of selecting a large dataset covering the whole
98 spectrum of feeding habits, we chose here to focus on four taxa representing four different
99 dietary poles (Table 1). These taxa are the hartebeest (*Alcelaphus buselaphus*, grazer; Estes,
100 1991; Gagnon and Chew, 2000), the red deer (*Cervus elaphus*, generalist; Gebert and
101 Verheyden-Tixier, 2001), the giraffe (*Giraffa* sp., leaf-dominant browser; Estes, 1991;
102 Leuthold, 1978; Parker et al., 2003) and the yellow-backed duiker (*Cephalophus silvicultor*;
103 fruit-dominant browser; Estes, 1991; Gagnon and Chew, 2000; Gauthier-Hion et al., 1980;
104 Lumpkin and Kranz, 1984). These ruminants share a common occlusal molar pattern. A fifth
105 modern species is included in this study: *Okapia johnstoni*, the okapi, assumed to be a
106 browser (Hart and Hart, 1989).

107 The taxonomy of the modern giraffe is currently under debate among zoologists.
108 Several subspecies of *Giraffa camelopardalis*, differing in their horns and coat
109 ornamentations had been identified (Brown et al., 2007; Groves and Grubb, 2011; Hassanin et
110 al., 2007; Kingdon et al., 2013; Wilson and Reeder, 2005) but a recent study based on multi-

111 locus DNA analysis recognizes the existence of four species (Fennessy et al., 2016): *G.*
112 *giraffa* (southern giraffe), *G. tippelskirchi* (Masai giraffe), *G. reticulata* (reticulated giraffe)
113 and *G. camelopardalis* (northern giraffe). The geographical distribution of the giraffe and its
114 genetic diversity were even higher until the Holocene since subfossil remains and glyph
115 representations in caves and rock shelters attest to its presence 4,000 years ago in north-
116 western Africa and along the Nile Valley (Le Quellec, 1999). Because of these taxonomic
117 uncertainties, we made the choice to group all modern giraffes under *Giraffa* sp. Our purpose
118 here is to have an ecologically homogeneous milestone to represent the leaf-dominant
119 browsing ecospace. None of the specimens of modern species used in this study were captive
120 before death, they were shot in the wild decades ago.

121 The fossil specimens belong to six genera: *Bohlinia*, *Helladotherium*, *Palaeogiraffa*,
122 *Palaeotragus* and *Samotherium*. The material comes from a dozen upper Miocene (Vallesian
123 and Turolian) localities in Greece, Bulgaria, Turkey, Afghanistan, Iran and Tunisia (Table 1,
124 Fig. 1). *Helladotherium duvernoyi* comes from the turolian faunas of Southern Bulgaria
125 (Geraads et al., 2005; Spassov, 2002), continental Greece (Kostopoulos et al., 1996;
126 Solounias, 1981), and southern Tunisia (but the identification there is less secure). The
127 specimens attributed to *Bohlinia attica* (Giraffinae) come from Nikiti-1 in Greece dated to
128 close to the Vallesian-Turolian transition (Kostopoulos, 2016) and from Kalimantsi (K),
129 Bulgaria (Geraads et al., 2005). Among the Palaeotraginae, the specimens assigned to
130 *Samotherium major* come from turolian sites: Mytilini-A, Mytilini-B (MTLA and MTLB; two
131 sites from the Mytilini ravines in Samos Island, Greece; Kostopoulos, 2009), Vathylakkos-3
132 (VAT) in the Axios Valley (Geraads, 1978), Salihpasalar (MYS) and erefköy-1 (MYSe-1) in
133 the Mu la Yata an Basin of Turkey (Kaya et al., 2012), and from the Turolian of
134 Mahmutgazi (MA) in Turkey (Sickenberg, 1975). The specimens of *S. boissieri* do not come
135 from recent excavations but belong to historical collections from Samos for which site

136 provenance is not guaranteed (see Koufos, 2009 for a historical review of the paleontological
137 surveys and studies in Samos). A single specimen attributed to *Samotherium neumayri* comes
138 from Maragha (MAR), Iran (Solounias and Danowitz, 2016, as *Alcicephalus neumayri*). The
139 genus *Palaeotragus* is represented by two taxa. A single specimen of *Palaeotragus rouenii*
140 from the vallesian site of Ravin de la Pluie (RPI; Geraads, 1978; Koufos, 2006) has been
141 analyzed but the species is widespread and abundant in the turolian sites of Hadjidimovo
142 (HD; Geraads et al., 2005), Dytiko-3 (DIT), Pikermi (PIK; Koufos, 2006), Mytilini-B
143 (MTLB; Kostopoulos, 2009), erefköy-1 and erefköy-2 (MYSe-1 and MYSe-2; Kaya et al.,
144 2012) and Molayan (MOL; Afghanistan; Brunet and Heintz, 1983; Sen, 1998). Specimens
145 that belong to *Palaeotragus coelophrys* or to a closely related species come from the vallesian
146 sites of Ravin de la Pluie (RPI) and Pentalophos (PNT) in Greece (Koufos, 2006) and from
147 Maragha (MAR) in Iran (Mecquenem, 1924; Solounias and Danowitz, 2016). *Palaeogiraffa*
148 *pamiri* comes from the vallesian sites of Küçükçekmece (KUC) in Turkish Thrace
149 (Kostopoulos and Sen, 2016). The only specimen of *Palaeogiraffa major* comes from the
150 vallesian site of Ravin de la Pluie (Koufos, 2006). A third species of *Palaeogiraffa*, *P.*
151 *macedoniae* is known from the vallesian site of Pentalophos (PNT), also in the Axios Valley
152 (Koufos, 2006). Ríos et al. (2016, 2017) synonymized *Palaeogiraffa* and *Decennatherium* (a
153 genus assumed to be the sister group of a clade composed notably by sivatherines and
154 *Samotherium major* and *S. boissieri*), a view which is not shared by Bonis & Bouvrain
155 (2003). Pending agreement on this taxonomic issue, we keep using *Palaeogiraffa* as genus
156 name for specimens from the vallesian sites from Axios, in northern Greece and from Yulafli,
157 in Turkish Thrace.

158 For some of the species, the number of specimens is large enough ($N \geq 10$) to generate
159 robust interpretations regarding their dietary habits. However, for several taxa, the number is
160 moderate ($5 \leq N < 10$) and even low ($5 < N$). Taking into account that dental microwear textures

161 reflect the dietary bolus from the last few weeks, one might fear that the signal from such
162 small samples is meaningless, but Purnell *et al.* (2012) have shown that significant differences
163 in textural parameters can be detected even for small samples ($N < 5$) of fishes (see also
164 Purnell *et al.*, 2013). Besides, the analysis of several scans per individual, as proposed by
165 Purnell and Darras (2016) and as done in the present study, mitigates the effects of the small
166 sample size..

167

168 2.2. *Methods*

169 DMTA is a method quantifying tooth abrasion (for detailed reviews of intra- and inter-
170 observer errors, see DeSantis *et al.*, 2013; Galbany *et al.*, 2005; Grine *et al.*, 2002;
171 Mihlbachler *et al.*, 2012; Calandra and Merceron, 2016; Mihlbachler and Beatty, 2012; Scott,
172 2012; Scott *et al.*, 2006) . Tooth wear reflects individual senescence and physical properties of
173 foods; thus, it is correlated with the availabilities of food resources and can be used to explore
174 niche partitioning among sympatric species of mammals (Calandra and Merceron, 2016).
175 From the scale of a whole tooth to the micrometric scars on dental facets, differences in
176 dietary preferences are mirrored by tooth wear. DMTA has proved to be a particularly useful
177 methodology free of (inter- and intra-)observer measurement errors at least at the analytic step
178 (for detailed reviews of intra- and inter-observer errors, see DeSantis *et al.*, 2013; Galbany *et*
179 *al.*, 2005; Grine *et al.*, 2002; Mihlbachler *et al.*, 2012; Mihlbachler and Beatty, 2012) in
180 assessing diets of fossil as well as modern taxa (Calandra and Merceron, 2016).

181 The analysis was performed preferentially on second upper or lower molars (Figs. 2
182 and 3). However, third or first molars were considered when the second molars are weathered,
183 too much worn or too recently erupted. Following standard procedures, replicas of dental
184 facet were produced with a silicone (medium consistency) polyvinylsiloxane (Coltène
185 Whaledent, President Regular Body, ISO 4823). Scans (320 x 280 μm) were produced on

186 replicas using a surface profilometer confocal DCM8 Leica Microsystems with a 100× lens
187 (Leica Microsystems; NA = 0.90; working distance = 0.9 mm) at the Paleovprim, CNRS and
188 University of Poitiers, France. Lateral resolution is 0.129 μm and vertical spacing is 0.002
189 μm. Up to four surfaces (140 × 100 μm; 1088 × 776 pixels) were generated from the original
190 scans and saved as .Plu files (Figs. 2 and 3; details on surface preparation are given in
191 Merceron et al. 2016).

192 The DMTA was performed using the Scale-Sensitive Fractal Analysis using Toothfrac
193 and Sfrac software (Surfract, <http://www.surfract.com>) following Scott et al. (2006). The
194 individual values of surface parameters for extinct and extant species are given in Appendix 1.
195 Three variables were extracted from the surface: complexity (Asfc), anisotropy (epLsar), and
196 heterogeneity of complexity (HAsfc calculated with a 9-cell mesh; Table 1). Scott et al.
197 (2006) detailed the variables used here. Complexity (Asfc or Area-scale fractal complexity) is
198 a measure of the roughness at a given scale. Anisotropy (epLsar or exact proportion of length-
199 scale anisotropy of relief) measures the orientation concentration of surface roughness.
200 Heterogeneity of complexity (HAsfc or heterogeneity of area-scale fractal complexity),
201 quantifies the variation of complexity within scan. All of these three textural parameters are
202 dimensionless (see Scott et al., 2006). Scanned surfaces display dental microwear but also, for
203 some of the teeth, structural reliefs such as growth lines or perikemata reflecting the
204 intersection between Retzius lines with the enamel surface. One may argue that such enamel
205 structural relief influences the parameter values, and notably the anisotropy of the dental
206 microwear textures. Although the perikemata are more or less preferentially orientated, they
207 do not interfere with the anisotropy calculation, because the height amplitudes of these
208 perikemata are lower than topographic variations due to the microwear on enamel surfaces
209 (Fig. 4).

210 As the distribution of textural parameters violates conditions for parametric tests,
211 variables were rank-transformed before analysis (Conover and Iman, 1981; Sokal and Rohlf,
212 1969). One-way factorial ANOVAs with post-hoc tests for each parameter were used to
213 determine the sources of significant variation (Tables 2 and 3). Any potential difference was
214 then highlighted using the combination of the conservative HSD test (Tukey's Honest
215 Significant Differences) together with the less conservative LSD test (Fisher's Least
216 Significant Differences).

217 Body mass (calculated according Scott, 1990) and height at the withers are two body
218 traits that can be used in combination with DMTA to explore the partitioning of food
219 resources between sympatric species. Here we use metacarpal length as a proxy of height at
220 the withers and the height at which a species can gather its resources. This certainly suffers
221 exceptions, but the length of the metacarpals is a good proxy for the height at which the
222 animal can browse (for a given metacarpal length, if the animal is heavier, height at the
223 withers will be higher, but neck will be shorter). We also noted classic parameters of dental
224 morphology, notably the premolar/molar ratio that is distinctly lower for hyper-grazing bovids
225 (Table 4).

226

227 **3. Results and Discussion**

228 *3.1. Dental microwear textures and diet*

229 The four modern species used as milestones differ from each other in all three surface
230 textural parameters (Tables 1-3). The hartebeest (*Alcelaphus buselaphus*), a grazing
231 alcelaphine, has the lowest enamel surface complexity (Asfc) and the highest anisotropy
232 (epLsar) of dental microwear textures (Tables 1 and 3; Figs. 2 and 4). The yellow-backed
233 duiker (*Cephalophus silvicultor*) displays the highest complexity (Asfc) and low values of
234 anisotropy (epLsar) whereas the giraffe (*Giraffa* sp.) has the lowest anisotropy (epLsar) and

235 an intermediate complexity (Asfc) between the hartebeest and the yellow-backed duiker
236 (Tables 1 and 3; Figs. 2 and 5). The differences in dental microwear textures between the two
237 browsing species reflect the ingestion of fruits and seeds by the duiker (Ramdarshan et al.,
238 2016). The dental microwear textures (intermediate complexity and anisotropy) of the red
239 deer (*Cervus elaphus*) reflect its mixed feeding habits that involve both browsing and grazing
240 (Tables 1 and 3; Figs. 2 and 5). The third variable, heterogeneity of complexity (HAsfc),
241 provides a significant complement. The giraffe and the hartebeest foraging mostly on a
242 homogeneous source of vegetation (tree leaves and herbaceous monocotyledons, respectively;
243 Estes, 1991, Gagnon and Chew, 2000; Leuthold, 1978; Parker et al., 2003) over long time
244 span (over a year) have lower values than the red deer and the yellow-backed duiker whose
245 diets are mechanically diverse and variable from a day to another or from a season to another
246 (Tables 1 and 3; Figs. 2 and 5; Estes, 1991; Gebert and Verheyden-Tixier, 2001; Gagnon and
247 Chew, 2000; Gauthier-Hion et al. 1980; Lumpkin and Kranz, 1984).

248 The modern okapi (*Okapia johnstoni*) has a wide distribution across the dental
249 microwear textural ecospace. It differs from the giraffe in having higher anisotropy (epLsar)
250 and from the yellow-backed duiker in having lower complexity (Asfc; Tables 1 and 3; Figs. 3
251 and 5). The okapi also differs from the hartebeest and the giraffe in having higher
252 heterogeneity of complexity (HAsfc). It does not differ from the red deer when the two most
253 discriminating variables (Asfc and epLsar) are considered (Tables 1 and 3; Figs. 3 and 5).
254 These results for the present-day okapi assumed to be a browser can be discussed in light of
255 the ecological data. Hitherto, only one single study dealt with the feeding ecology of the okapi
256 in the wild (Hart and Hart, 1989). It was conducted at Epulu, Ituri forest, a lowland forest
257 located at the far north eastern of the Congo basin. The authors tracked eight collared
258 individuals for several months and recorded from direct observations browse signs on
259 vegetation but only those ranging from 0.5 to 2.0 meters in height because *õthis is the forest*

260 *layer most frequently browsed by okapiö* (Hart and Hart, 1989: 35). There is indeed no record
261 regarding lower vegetal layers. Hart and Hart (1989) identified shade- and light-tolerant plant
262 species, all of them being dicotyledonous trees or bushes, constituting the staple food
263 spectrum of the okapi. However, one of these two authors from the pioneer study mentions in
264 Kingdon et al. (2013: in vol. VI, p. 110-115) that herbaceous monocotyledons are part of the
265 okapi diet but does not provide details regarding their abundance. Hart and Hart (1989) had
266 actually made mention that the okapi favors tree-fall gaps where it leaves the highest density
267 of browse signs. These tree-fall gaps are also hotspots of biodiversity in the Central African
268 forest where the herbaceous vegetation (mostly monocotyledons) reaches its highest diversity
269 and density. These plant resources are known to be critical in dense forested habitats for other
270 mammals such as buffaloes (Blake, 2002), gorillas, and pygmy chimpanzees (Blake et al.,
271 1995; Malenky and Wrangham, 1994; Williamson et al., 1990). For instance, these apes feed
272 on herbaceous stems (sometimes only the soft inner pith) of monocotyledonous plants such as
273 Marantacea and Zingiberacea (Malenky and Wrangham, 1994; Williamson et al., 1990;
274 Wrangham et al., 1991). Monocotyledonous plants have generally higher silica content than
275 dicotyledonous plants (Hodson et al., 2005). Besides, the herbaceous stems that are eaten are
276 tougher than most fruits (Elgart-Berry, 2004). Therefore, on the basis of the dental microwear
277 textures of the okapis analyzed in the present study and the information provided by Hart and
278 Hart (1989) and Hart in Kingdon et al. (2013), we hypothesize that the okapi does include
279 some terrestrial herbaceous vegetation in its diet, especially when its home range overlaps tree
280 fall gaps. Our hypothesis needs to be tested in the future through alternative direct or non
281 direct dietary proxies and new material. It is worth mentioning that Clauss et al. (2006) had
282 described the digestive tract of two captive okapis as similar to that of modern selective
283 browsers with the exception that the parotid glands were found to be small, a feature shared
284 with ruminants feeding on monocotyledons.

285 All fossil giraffids but *Samotherium boissieri* (and the only specimen of *Palaeogiraffa*
286 *major*, see Table 1) significantly differ from the grazing hartebeest in having either higher
287 complexity (Asfc) or lower anisotropy (epLsar) or the combination of the two conditions
288 (Tables 2 and 3; individual values are provided in table S1 in supplementary material). Like
289 the modern giraffe, *Helladotherium duvernoyi* has lower anisotropy (epLsar) than the red deer
290 and the hartebeest, and lower complexity (Asfc) than the yellow-backed duiker; it also has
291 lower values in heterogeneity of complexity (HAsfc) than the red deer and the duiker,
292 supporting a monotypic diet for this sivatheriine (Tables 1 and 3; Figs. 3 and 5; table S1).
293 There is little doubt that *Helladotherium* (N= 15) was a leaf-dominant browser. The five
294 specimens of *Bohlinia attica* all have low values of both anisotropy (epLsar) and complexity
295 (Asfc) suggesting that these individuals fed on soft browse (Tables 1 and 3; Figs. 3 and 5;
296 table S1). The specimens of *Palaeogiraffa pamiri* from Turkish Thrace show low values in all
297 three textural parameters (Tables 1 and 3; Figs. 3 and 5; table S1), showing that they were
298 undoubtedly leaf-dominated browsers. By contrast, *Palaeogiraffa macedoniae* and the
299 specimen of *P. major* from the Axios Valley sites in northern Greece display a sharply
300 different pattern (Tables 1 and 3; Fig. 3; table S1). They have higher anisotropy (epLsar) than
301 the sample from Thrace, the modern giraffe and the yellow-backed duiker. When complexity
302 (Asfc) is also considered, such dental microwear textures suggest mixed feeding habits for
303 *Palaeogiraffa* from the lower Axios Valley (Tables 1 and 3; Fig. 5; table S1). One may argue
304 that differences in windblown dust deposit on vegetation could be the key factor controlling
305 differences in dental microwear textures. However the only study that actually tested these
306 hypotheses on living captive domesticated animals concludes that differences in (dust-free)
307 diet generates significant differences in dental microwear textures (Merceron et al., 2016).
308 Moreover, the effects on foods of dust simulating the Western Africa Harmattan windblown
309 dust are not significant enough to hide the dietary signal (Merceron et al., 2016). *Samotherium*

310 also displays a wide range of values (Tables 1 and 3; Figs. 3 and 5; table S1). *Samotherium*
311 *major* differs from the modern giraffe in having higher anisotropy (epLsar), from the
312 hartebeest in having a higher complexity (Asfc) and from the red deer, the yellow-backed
313 duiker, and the okapi in its lower heterogeneity of complexity (HAsfc; Tables 1 and 3; Figs. 3
314 and 5; table S1). *Samotherium boissieri* also has higher anisotropy (epLsar) than the giraffe
315 and the yellow-backed duiker. It is worth noting that there is no significant difference between
316 *S. boissieri* and the grazing and mixed feeding species. The sample of *Palaeotragus rouenii*
317 displays higher anisotropy (epLsar) than the modern giraffe and lower complexity (Asfc) than
318 the yellow-backed duiker. This species covers the whole spectrum. cf. *P. coelophrys* shares
319 the same pattern. On the whole, mixed feeding habits seem to be prevalent for all
320 palaeotragines.

321

322 3.2. Morphology, diet, and niche partitioning

323 Modern giraffids constitute a relic of a diverse group that became impoverished during
324 Pliocene and Pleistocene times, but during the late Miocene, their species and
325 ecomorphological diversities were far greater than today. Body mass and heights at which
326 they could gather food resources differed from one species to another (Table 4, Fig. 6).
327 *Helladotherium duvernoyi* was likely the heaviest giraffe in Europe, weighting perhaps as
328 much as two tons, whereas *Palaeotragus rouenii* was not larger than the modern okapi, at
329 about 500 kg. The length of their metacarpals, approximating height at the withers, and the
330 height at which each species could reach its food, covered the whole range of the modern
331 forms, from the okapi to the giraffe. The relative proportions of the premolar / molar rows are
332 not very variable in the Giraffidae, which suggests that there were probably no huge
333 differences in diets. On the basis of the index (Table 4, Fig. 6), and given low sample size,
334 most fossil giraffes do not significantly differ from their modern relatives, except the

335 paleotragines that have smaller premolars. This is in agreement with the dental microwear
336 textural analysis that suggests more versatile feeding habits for paleotragines than other
337 extinct giraffids.

338 *Bohlinia attica* was a giraffine weighting about a ton; it was likely able to reach
339 foliage as high as the modern giraffe, from 4 to 6 m above ground (Table 4, Fig. 6; Leuthold,
340 1978; O'Connor et al., 2015). The dental microwear textures attest that *B. attica* fed mostly on
341 soft foliages, as modern giraffes do (Figs. 5 and 6). The body traits found in *Bohlinia* and
342 *Giraffa* and their similarities in tooth wear both suggest that the ecological niche of leaf-
343 dominated browsers targeting the highest tree foliages was shared by the common ancestor.

344 Among large giraffids, the sivatheriine *Helladotherium duvernoyi* weighted as much
345 as two tons; the low values for the three textural parameters depict it as a likely leaf-dominant
346 browser (Fig. 5). Thus, *H. duvernoyi* shared similar feeding habits with *B. attica*, in spite of
347 its distinctly higher molar crowns (Table 4), but could not reach foliages as high as this
348 species, which was less stoutly built, but taller (Table 4, Fig. 6). *Palaeogiraffa* is represented
349 in this study by three species. They were less tall than *B. attica*, and thus had reduced
350 competition with it to exploit tree foliages (Fig. 6). *Palaeogiraffa pamiri* from Thrace was
351 likely a leaf-dominant browser while the contemporaneous *P. macedoniae* and *P. major* from
352 the lower Axios valley in Greece may have incorporated herbaceous monocotyledons in their
353 diet. Such contrasted differences between species of the same genus (Figs. 5 and 6) might
354 reflect differences in food resources between the two regions (woody landscapes in the
355 Thracian site and floodplain grasslands along the Axios).

356 In the late Miocene of the Mediterranean region, palaeotragines were more diverse
357 than sivatheriines and giraffines, but the height range at which they could browse is far
358 smaller than their species diversity and body mass range suggest. The palaeotragine
359 *Samotherium major* has a body mass similar to that of the sivatheriine *H. duvernoyi* (Table 4,

360 Fig. 6). These two species could reach the same foliage heights. Based on tooth morphology,
361 we would have expected more grazing habits for the large palaeotragine compared to the
362 sivatheriine, because small premolars compared to molars are usually taken as indicating
363 more grazing habits in ruminants (Solounias and Dawson-Saunders, 1988), but no significant
364 difference in the present study seems to distinguish the species with the larger premolars (*H.*
365 *duvernoyi*) from the similar-sized species with the smaller premolars (*S. major*; Table 4, Figs.
366 5 and 6). However, using dental microwear analysis on a larger sample, Solounias et al.
367 (2010) regarded *S. major* as a mixed feeder. Based on a dental mesowear scoring approach,
368 Danowitz et al. (2016) depicted it as a browser or a mixed feeder. To sum up, although the
369 present study fails to discriminate *S. major* from *H. duvernoyi*, previous studies supported the
370 view that *S. major* included herbaceous monocotyledons in its diet, as suggested by its dental
371 morphology.

372 *Samotherium boissieri* differs from *S. major* in its lighter body mass and in being less
373 tall at the withers. Besides, the slight differences in the morphology of the premaxilla (but not
374 in the teeth) between these co-generic species (Fig. 7) suggest that *S. boissieri* might have
375 ingested more herbaceous monocotyledons than *S. major*, although according to our own
376 observation, the specimen NHMUK M 4215 has a distinctly less squarish premaxilla than
377 typical grazers. Although our study fails to detect any significant differences between these
378 two species of *Samotherium*, it is worth mentioning that, in contrast to *S. major*, *S. boissieri*
379 has significantly higher values of anisotropy than modern browsing species (yellow-backed
380 duiker and giraffe) and the three most presumably leaf browsing extinct giraffids (*B. attica*, *H.*
381 *duvernoyi*, *P. pamiri*; Table 4, Figs. 5 and 6). Solounias et al. (1988) had also shown that *S.*
382 *boissieri* includes herbaceous monocotyledons in its diet.

383 The genus *Palaeotragus* is represented by two species. *Palaeotragus rouenii* has a
384 body mass similar to that of the modern okapi but could reach vegetal layers as high as those

385 that *H. duvernoyi* and *Samotherium* spp. browsed (Table 4, Fig. 6). A more versatile diet than
386 that of *H. duvernoyi* could explain their coexistence at some sites, and thus the probable
387 overlap of their home ranges. *Palaeotragus coelophrys* was stouter than *P. rouenii*, but based
388 on their metacarpal lengths, they could reach the same foliages. A fifth species of
389 palaeotragine, *Samotherium neumayri*, is represented by a single individual whose body mass
390 was similar to that of the modern giraffe but with a height at the withers similar to that of
391 other palaeotragines; its dental microwear texture suggests that this specimen fed on soft
392 foliages the few weeks before its death.

393

394 3.3 Dietary adaptation and Phylogeny

395 A recent study based on new material challenges the phylogeny of the giraffids (Ríos
396 et al., 2017). Giraffines are represented by the modern giraffes and the species of the genus
397 *Bohlinia*. The elongation of the cervical vertebrae and the extreme elongation of the
398 metacarpal allowing them to forage on the highest arboreal stratum may be seen as an
399 autapomorphy of the Giraffinae (Ríos et al., 2017). Our data strongly support such dietary
400 adaptations. Besides, the monophyly of the paleotragines is challenged. According to their
401 study, the genus *Samotherium*, previously thought to be close to *Palaeotragus*, actually shares
402 a set of derived features with the Sivatherinae. The species of the genus *Palaeotragus*
403 compose the sister group of a monophyletic group including the modern okapi,
404 *Decennatherium*, *Palaeogiraffa* (assumed to be close to the former genus according to these
405 authors) and *Samotherium* in which the sivatherines (including *Helladotherium*) are rooted.
406 More versatile feeding habits might have been the ancestral conditions for this second clade.
407 In view of this phylogeny proposed by Ríos et al. (2017), we may consider that either
408 browsing or mixed feeding habits were the ancestral ecological conditions for giraffids. The
409 adaptation to leaf browsing occurred twice, first among Giraffines and then at least in

410 *Helladotherium* within the Sivatherines. It is worth mentioning that the African sivatheres
411 show a shortening of the forelimbs in the course of the Pliocene, a morphological trend
412 correlated with the incorporation of a greater amount of C₄ plants, i.e. herbaceous monocots,
413 in their diet.

414

415 **4. Conclusions**

416 The present study explores the ecological diversity of the diverse radiation of giraffids
417 that took place during the late Miocene of the Eastern Mediterranean. In combination with
418 body traits such as wither heights, and thus estimation of the height at which these extinct
419 ruminants may have foraged, DMTA detects differences in feeding preferences. As expected,
420 several of these extinct giraffids were leaf-dominant browsers but foraging at different
421 heights. The modern giraffe can be consider as an appropriate model for understanding the
422 ecology of *Bohlinia*. *Helladotherium duvernoyi* browsed at lower heights. Our study supports
423 previous views that regarded the species of *Samotherium* as engaged in both browsing and
424 grazing. *Palaeogiraffa* from the Axios valley in Greece undoubtedly included high amounts
425 of tough plants, most likely tall herbaceous monocots, in its diet. The present study enlarges
426 our knowledge of the ecology of this diversified group and emphasizes the importance of
427 considering megaherbivores to faithfully depict past ecosystems and available resources.
428 Indeed, together with proboscideans, rhinocerotids and chalicotheriids, giraffids compose a
429 guild of megaherbivores with no analog in the modern ecosystems.

430 In addition, the present study provides surprising results regarding the okapi. Its dental
431 microwear textures significantly differ from those of the leaf-eating giraffes as well as from
432 those of the fruit-eating yellow-backed duikers. They show similarities with those of the red
433 deer, a species eating both monocots and dicots. Here, we hypothesize that the okapi is not a
434 browser *sensu stricto*. This giraffid feeds on a wider dietary spectrum than previously thought
435 and likely forages on tough plants, possibly tall herbaceous monocotyledons when exploiting
436 resources in tree fall gaps.

437

438 **5. Acknowledgments**

439 The authors thank C. Sagne and P. Tassy (Muséum National d'Histoire Naturelle,
440 Paris, France), E. Robert (Geological Collections, UMR CNRS 5276 Laboratoire de Géologie
441 de Lyon - CERESE, University Lyon 1), N. Spassov and the late D. Kovatchev (National
442 Museum of Natural History, Sofia, Bulgaria), D.S. Kostopoulos and G.D. Koufos (Aristotle
443 University of Thessaloniki, Greece), S. Mayda and T. Kaya (Natural History Museum, Ege
444 University, Izmir, Turkey), W. Wendelen (RMCA, Tervuren, Belgium), L. Costeur
445 (Naturhistorisches Museum at Basel, Switzerland), and W. Munk (Staatliches Museum für
446 Naturkunde, Karlsruhe, Germany), for giving access to collections. We are grateful to A.
447 Souron (University of Bordeaux-1) who contributed to the sampling of okapis.

448 A significant part of the fossil material was sampled in various European institutions
449 thanks to the International Research Collaborative Grant "*Environmental Dynamics of*
450 *Western Eurasian Hominids during the Late Miocene*" (PIs: R. S. Scott and T. Kaya) funded
451 by the Wenner-Gren Foundation. G.M. thanks his colleagues of the Wenner-Gren
452 International Research Collaborative Grant group: R.S. Scott (Rutgers University, USA),
453 D.S. Kostopoulos (Aristotle University of Thessaloniki, Greece), T. Kaya and S. Mayda (Ege
454 University, Izmir, Turkey) as well as G. Reynaud and S. Riffaut (Paleovprim). We also thanks
455 the associate editor I. Montanez and four reviewers including N. Spassov for their helpful
456 comments that greatly improve the manuscript. This study was funded by the Project
457 TRIDENT (ANR-13-JSV7-0008-01, PI: G. Merceron, France; <http://anr-trident.prd.fr/>).

458

459 **6. Data availability**

460 The dental microwear texture parameters for each fossil specimen are given in Appendix 1.

461 **6. References**

- 462 Blake, S., 2002. Forest buffalo prefer clearings to closed-canopy forest in the primary forest
463 of northern Congo. *Oryx* 36, 81686.
- 464 Blake, S., Rogers, E., Fay, J.M., Ngangoué, M., Ebéké, G., 1995. Swamp gorillas in northern
465 Congo. *Afr. J. Ecol.* 33, 2856290. <https://doi.org/10.1111/j.1365-2028.1995.tb00809.x>
- 466 Bonis, L. de, Bouvrain, G., 2003. Nouveaux Giraffidae du Miocène supérieur de Macédoine
467 (Grèce). *Adv. Vertebr. Paleontol. ðHen Panta* 5616.
- 468 Brown, D.M., Breneman, R.A., Koepfli, K.-P., Pollinger, J.P., Milá, B., Georgiadis, N.J.,
469 Louis, E.E., Grether, G.F., Jacobs, D.K., Wayne, R.K., 2007. Extensive population genetic
470 structure in the giraffe. *BMC Biol.* 5, 1.
- 471 Brunet, M., Heintz, E., 1983. Interprétation paléoécologique et relations biogéographiques de
472 la faune de vertébrés du Miocène supérieur dInjana, Irak. *Palaeogeogr. Palaeoclimatol.*
473 *Palaeoecol.* 44, 2836293.
- 474 Calandra, I., Merceron, G., 2016. Dental microwear texture analysis in mammalian ecology:
475 DMTA in ecology. *Mammal Rev.* 46, 2156228. <https://doi.org/10.1111/mam.12063>
- 476 Clauss, M., Hummel, J., Völlm, J., Lorenz, A., Hofmann, R.R., 2006. The allocation of a
477 ruminant feeding type to the okapi (*Okapia johnstoni*) on the basis of morphological
478 parameters. *Zoo Anim. Nutr.* 3, 2536270.
- 479 Colbert, E.H., 1938. The relationships of the okapi. *J. Mammal.* 19, 47664.
- 480 Conover, W.J., Iman, R.L., 1981. Rank transformations as a bridge between parametric and
481 nonparametric statistics. *Am. Stat.* 35, 1246129.
- 482 Danowitz, M., Hou, S., Muhlbachler, M., Hastings, V., Solounias, N., 2016. A combined-
483 mesowear analysis of late Miocene giraffids from North Chinese and Greek localities of the
484 Pikermian Biome. *Palaeogeogr. Palaeoclimatol. Palaeoecol.* 449, 1946204.

485 DeSantis, L.R.G., Scott, J.R., Schubert, B.W., Donohue, S.L., McCray, B.M., Van Stolk,
486 C.A., Winburn, A.A., Greshko, M.A., O'Hara, M.C., 2013. Direct Comparisons of 2D and 3D
487 Dental Microwear Proxies in Extant Herbivorous and Carnivorous Mammals. PLoS ONE 8,
488 e71428. <https://doi.org/10.1371/journal.pone.0071428>

489 Elgart-Berry, A., 2004. Fracture toughness of mountain gorilla (*Gorilla gorilla beringei*) food
490 plants. Am. J. Primatol. 62, 2756285. <https://doi.org/10.1002/ajp.20021>

491 Estes, R.D., 1991. Behavior Guide to African mammals. The University of California Press,
492 Los Angeles.

493 Fennessy, J., Bidon, T., Reuss, F., Kumar, V., Elkan, P., Nilsson, M.A., Vamberger, M., Fritz,
494 U., Janke, A., 2016. Multi-locus Analyses Reveal Four Giraffe Species Instead of One. Curr.
495 Biol. <https://doi.org/10.1016/j.cub.2016.07.036>

496 Gagnon, M., Chew, A.E., 2000. Dietary preferences in extant African Bovidae. J. Mammal. 8,
497 4906511.

498 Galbany, J., Martínez, L.M., López-Amor, H.M., Espurz, V., Hiraldo, O., Romero, A., de
499 Juan, J., Pérez-Pérez, A., 2005. Error rates in buccal-dental microwear quantification using
500 scanning electron microscopy. Scanning 27, 23629. <https://doi.org/10.1002/sca.4950270105>

501 Gauthier-Hion, A., Emmons, L.H., Dubost, G., 1980. A comparison of the diets of three major
502 groups of primary consumers of Gabon (Primates, Squirrels and Ruminants). Oecologia 45,
503 1826189.

504 Gebert, C., Verheyden-Tixier, H., 2001. Variations of diet composition of red deer (*Cervus*
505 *elaphus* L.) in Europe. Mammal Rev. 31, 1896201.

506 Geraads, D., 1989. Vertébrés fossiles du Miocène supérieur du Djebel Krechem El Artsouma
507 (Tunisie centrale). Comparaisons biostratigraphiques. Géobios 22, 7776801.

508 Geraads, D., 1986. Remarques sur la systématique et la phylogénie des Giraffidae
509 (Artiodactyla, Mammalia). Geobios 19, 4656477.

510 Geraads, D., 1978. Les Paleotraginae (Giraffidae, Mammalia) du Miocène supérieur de la
511 région de Thessalonique (Grèce). Géologie Méditerranéenne V, 269-276.

512 Geraads, D., Spassov, N., Kovachev, D., 2005. Giraffidae (Artiodactyla, Mammalia) from the
513 Late Miocene of Kalimantsi and Hadjidimovo, Southwestern Bulgaria. Geol. Balc. 35, 11-18.

514 Grine, F.E., Ungar, P.S., Teaford, M.F., 2002. Error rates in dental microwear quantification
515 using scanning electron microscopy. Scanning 24, 144-153.
516 <https://doi.org/10.1002/sca.4950240307>

517 Groves, C., Grubb, P., 2011. Ungulate taxonomy. JHU Press.

518 Hart, J.A., Hart, T.B., 1989. Ranging and feeding behaviour of okapi (*Okapia johnstoni*) in
519 the Ituri Forest of Zaire: food limitation in a rain-forest herbivore, in: Symposium of the
520 Zoological Society of London. pp. 31-50.

521 Hassanin, A., Ropiquet, A., Gourmand, A.-L., Chardonnet, B., Rigoulet, J., 2007.
522 Mitochondrial DNA variability in *Giraffa camelopardalis*: consequences for taxonomy,
523 phylogeography and conservation of giraffes in West and central Africa. C. R. Biol. 330, 265-
524 274.

525 Hodson, M.J., White, P.J., Mead, A., Broadley, M.R., 2005. Phylogenetic variation in the
526 silicon composition of plants. Ann. Bot. 96, 1027-1046.

527 Kaya, T.T., Mayda, S., Kostopoulos, D.S., Alcicek, M.C., Merceron, G., Tan, A., Karakutuk,
528 S., Giesler, A.K., Scott, R.S., 2012. Irefköy-2, a new late Miocene mammal locality from
529 the Yata an Formation, Mu la, SW Turkey. Comptes Rendus Palevol 11, 5-12.

530 Kingdon, J., Happold, D., Butynski, T., Hoffmann, M., Happold, M., Kalina, J., 2013.
531 Mammals of Africa. A&C Black.

532 Kostopoulos, D.S., 2016. Palaeontology of the upper Miocene vertebrate localities of Nikiti
533 (Chalkidiki Peninsula, Macedonia, Greece): Artiodactyla. Geobios 49, 119-134.

534 Kostopoulos, D.S., 2009. The Late Miocene mammal faunas of the Mytilinii Basin, Samos
535 Island, Greece: new collection. 13. Giraffidae. Beitr. Zur Paläontol. 31, 299-343.

536 Kostopoulos, D.S., Koliadimou, K.K., Koufos, G.D., 1996. The giraffids from the Late
537 Miocene mammalian localities of Nikiti (Macedonia, Greece). Palaeontogr. Abt. -Stuttg.- 239,
538 61-688.

539 Kostopoulos, D.S., Sen, S., 2016. Suidae, Tragulidae, Giraffidae, and Bovidae. Geodiversitas
540 38, 273-298.

541 Koufos, G.D., 2009. The Late Miocene mammal faunas of the Mytilinii Basin, Samos Island,
542 Greece: new collection. 1. History of the Samos Fossil Mammals. Beitr. Zur Paläontol. 31, 1-
543 12.

544 Koufos, G.D., 2006. The Neogene mammal localities of Greece: faunas, chronology and
545 biostratigraphy. Hell. J. Geosci. 41, 183-214.

546 Le Quellec, J.-L., 1999. Répartition de la grande faune sauvage dans le nord de l'Afrique
547 durant l'Holocène. Anthropol.-PARIS- 103, 161-176.

548 Leuthold, B.M., 1978. Ecology of the giraffe in Tsavo East National Park, Kenya. East Afr.
549 Wildl. J. 16, 1-20.

550 Lumpkin, S., Kranz, K.R., 1984. *Cephalophus sylvicultor*. Mamm. Species 225, 1-7.

551 Malenky, R.K., Wrangham, R.W., 1994. A quantitative comparison of terrestrial herbaceous
552 food consumption by *Pan paniscus* in the Lamako forest, Zaire, and *Pan troglodytes* in the
553 Kibale forest, Uganda. Am. J. Primatol. 32, 1-12.

554 Mecquenem, R. de, 1924. Contribution à l'étude des fossiles de Maragha. Ann. Paléontol.
555 Vertébrés 13/14, 135-160.

556 Merceron, G., Ramdarshan, A., Blondel, C., Boisserie, J.-R., Brunetiere, N., Francisco, A.,
557 Gautier, D., Milhet, X., Novello, A., Pret, D., 2016. Untangling the environmental from the
558 dietary: dust does not matter. Proceeding R. Soc. Lond. B 283, 20161032.

559 Mihlbachler, M.C., Beatty, B.L., 2012. Magnification and resolution in dental microwear
560 analysis using light microscopy. *Paleontol Electron.* 15, 25A.

561 Mihlbachler, M.C., Beatty, B.L., Caldera-Siu, A., Chan, D., Lee, R., 2012. Error rates and
562 observer bias in dental microwear analysis using light microscopy. *Palaeontol. Electron.* 15,
563 12A.

564 O'Connor, D.A., Butt, B., Fouvopoulos, J.B., 2015. Foraging ecologies of giraffe (*Giraffa*
565 *camelopardalis reticulata*) and camels (*Camelus dromedarius*) in northern Kenya: effects of
566 habitat structure and possibilities for competition? *Afr. J. Ecol.* 53, 1836193.
567 <https://doi.org/10.1111/aje.12204>

568 Parker, D.M., Bernard, R.T.F., Colvin, S.A., 2003. The diet of a small group of extralimital
569 giraffe. *Afr. J. Ecol.* 41, 245.

570 Purnell, M., Seehausen, O., Galis, F., 2012. Quantitative three-dimensional microtextural
571 analyses of tooth wear as a tool for dietary discrimination in fishes. *J. R. Soc. Interface* 9,
572 222562233.

573 Purnell, M.A., Crumpton, N., Gill, P.G., Jones, G., Rayfield, E.J., 2013. Within-guild dietary
574 discrimination from 3-D textural analysis of tooth microwear in insectivorous mammals. *J.*
575 *Zool.* 291, 2496257.

576 Purnell, M.A., Darras, L.P.G., 2016. 3D tooth microwear texture analysis in fishes as a test of
577 dietary hypotheses of durophagy. *Surf. Topogr. Metrol. Prop.* 4, 014006.
578 <https://doi.org/10.1088/2051-672X/4/1/014006>

579 Ramdarshan, A., Blondel, C., Brunetière, N., Francisco, A., Gautier, D., Surault, J., Merceron,
580 G., 2016. Seeds, browse, and tooth wear: a sheep perspective. *Ecol. Evol.* 6, 555965569.

581 Ríos, M., Sánchez, I.M., Morales, J., 2017. A new giraffid (Mammalia, Ruminantia, Pecora)
582 from the late Miocene of Spain, and the evolution of the sivathere-samothere lineage. *PLOS*
583 *ONE* 12, e0185378. <https://doi.org/10.1371/journal.pone.0185378>

584 Ríos, M., Sánchez, I.M., Morales, J., 2016. Comparative anatomy, phylogeny, and
585 systematics of the Miocene giraffid *Decennatherium pachecoi* Crusafont, 1952 (Mammalia,
586 Ruminantia, Pecora): State of the art. J. Vertebr. Paleontol. 36, e1187624.
587 <https://doi.org/10.1080/02724634.2016.1187624>

588 Scott, J.R., 2012. Dental microwear texture analysis of extant African Bovidae. Mammalia 76,
589 1576174.

590 Scott, K.M., 1990. Postcranial dimensions of ungulates as predictors of body mass. Body Size
591 Mamm. Paleobiology Estim. Biol. Implic. 30, 16335.

592 Scott, R.S., Ungar, P., Bergstrom, T.S., Brown, C.A., Childs, B.E., Teaford, M.F., Walker, A.,
593 2006. Dental microwear texture analysis: technical considerations. J. Hum. Evol. 51, 3396
594 349.

595 Sen, S., 1998. The age of the Molayan mammals locality, Afghanistan. Geobios 31, 3856391.

596 Senyürek, M.S., 1954. A study of the remains of *Samotherium* found at - Recherche Google.
597 Rev. Fac. Lang. Hist. Géographie Univ. Ank. 12, 1632.

598 Sickenberg, O., 1975. Die Gliederung des höheren Jungtertiärs und Altquartärs-in der Türkei
599 nach Vertebraten und ihre Bedeutung für die-internationale Neogen-Gliederung. Geol. Jahrb.
600 Reihe B 16167.

601 Sokal, S.R., Rohlf, F.J., 1969. Biometry. W. E. Freeman and Company, New York.

602 Solounias, N., 1988. Evidence from horn morphology on the phylogenetic relationship of the
603 Pronghorn (*Antilocapra americana*). J. Mammal. 69, 1406143.

604 Solounias, N., 1981. Mammalian fossils of Samos and Pikermi. Part 2. Resurrection of a
605 classic turolian fauna. Ann. Carnegie Mus. 50, 2316269.

606 Solounias, N., Danowitz, M., 2016. The Giraffidae of Maragheh and the identification of a
607 new species of *Honanotherium*. Palaeobiodiversity Palaeoenvironments 96, 489-506.

608 Solounias, N., Dawson-Saunders, B., 1988. Dietary adaptations and paleoecology of the late
609 Miocene ruminants from Pikermi and Samos in Greece. *Palaeogeogr. Palaeoclimatol.*
610 *Palaeoecol.* 65, 149-172.

611 Solounias, N., Mac Graw, W.S., Hayek, L.-A., Werdelin, L., 2000. The paleodiet of the
612 Giraffidae, in: Vrba, E.S., Schaller, G.B. (Eds.), *Antelopes, Deer, and Relatives*. Yale
613 University Press, New Haven, pp. 84-95.

614 Solounias, N., Rivals, F., Semprebon, G.M., 2010. Dietary interpretation and paleoecology of
615 herbivores from Pikermi and Samos (late Miocene of Greece). *Paleobiology* 36, 113-136.
616 <https://doi.org/10.1666/0094-8373-36.1.113>

617 Solounias, N., Teaford, M.F., Walker, A., 1988. Interpreting the diet of extinct ruminants : the
618 case of a non-browsing giraffid. *Paleobiology* 14, 287-300.

619 Spassov, N., 2002. The Turolian Megafauna of West Bulgaria and the character of the Late
620 Miocene -Pikermian biome. *Bull. Della Soc. Paleontol. Ital.* 41, 69-81.

621 Thenius, E., 1992. Das Okapi (Mammalia, Artiodactyla) von Zaire - šlebendes Fossilö oder
622 sekundärer Urwaldbewohner? *J. Zool. Syst. Evol. Res.* 30, 163-179.
623 <https://doi.org/10.1111/j.1439-0469.1992.tb00166.x>

624 Williamson, E.A., Tutin, C.E.G., Rogers, M.E., Fernandez, M., 1990. Composition of the diet
625 of lowland gorillas at Lopé in Gabon. *Am. J. Phys. Anthropol.* 21, 265-277.

626 Wilson, D.E., Reeder, D.M., 2005. *Mammal species of the world: a taxonomic and*
627 *geographic reference*. JHU Press.

628 Wrangham, R.W., Conklin, N.L., Chapman, C.A., Hunt, K.D., 1991. The significance of
629 fibrous foods for Kibale forest chimpanzees. *Philos. Transl. R. Soc. Lond.* 334, 171-178.

630

631

632 **Table 1.** Descriptive statistics of dental microwear textural parameters of modern ruminants
 633 and extinct species of giraffids.

	Taxa	N	Asfc*		epLsar ($\times 10^{-3}$)		HAsfc	
			m	sd	m	sd	m	sd
Modern species	<i>Cephalophus silvicultor</i>	25	4.03	3.25	3.07	1.58	0.54	0.30
	<i>Giraffa</i> sp.	12	2.51	1.48	2.10	1.57	0.35	0.12
	<i>Cervus elaphus</i>	29	2.12	0.80	4.59	1.91	0.55	0.25
	<i>Okapia johnstoni</i>	25	2.46	1.46	4.07	2.07	0.52	0.27
	<i>Alcelaphus buselaphus</i>	28	1.60	0.77	5.80	1.64	0.39	0.12
Extinct species	<i>Bohlinia attica</i>	5	1.47	0.73	2.47	0.94	0.49	0.11
	<i>Helladotherium duvernoyi</i>	15	2.46	1.23	2.99	1.37	0.43	0.52
	<i>Palaeogiraffa macedoniae</i>	6	2.61	0.65	5.13	2.63	0.36	0.14
	<i>Palaeogiraffa major</i>	1	2.87	-	6.41	-	0.38	-
	<i>Palaeogiraffa paimiri</i>	6	1.68	0.93	1.92	0.97	0.51	0.29
	<i>Samotherium neumayri</i>	1	0.66	-	1.99	-	0.15	-
	<i>Palaeotragus rouenii</i>	21	2.30	1.06	3.80	1.63	0.35	0.11
	cf. <i>P. coelophrys</i>	3	1.84	0.93	3.60	2.43	0.34	0.07
	<i>Samotherium boissieri</i>	5	2.43	1.33	4.97	2.10	0.37	0.14
	<i>Samotherium major</i>	9	2.89	1.63	3.70	1.63	0.37	0.25

634

635 * all of these three parameters are dimensionless (see Scott et al., 2006); m: mean; sd: standard deviation; Asfc:
 636 complexity; epLsar: anisotropy (calculated at the 1.8 μm scale); HAsfc: Heterogeneity of complexity (calculated
 637 with a 9-cell mesh).

638 **Table 2.** Analysis of variance on rank-transformed variables.

639

	<i>df</i>	SS	MS	F	<i>p</i>
Asfc	14	115848.3	8274.9	3.1334	0.0002
	176	464791.7	2640.9		
epLsar	<i>df</i>	SS	MS	F	<i>P</i>
	14	176760.3	12625.7	5.5020	0.0000
	176	403878.7	2294.8		
HAsfc	<i>df</i>	SS	MS	F	<i>P</i>
	14	109086.9	7791.9	2.9082	0.0005
	176	471552.1	2679.3		

640 Asfc: complexity; epLsar: anisotropy (calculated at the 1.8 μm scale); HAsfc: Heterogeneity of complexity

641 (calculated with a 9-cell mesh). ; SS: sum of squares; MS: mean of squares; F: F statistic; p: p-value

642

643 Table 3. Post-hoc test of comparisons (the Fisher Least Significant Differences and the
 644 conservative Tukey Honest Significant Differences test).

	<i>C. silvicultor</i>	<i>C. elaphus</i>	<i>Giraffa</i> sp.	<i>O. johnstoni</i>	<i>A. buselaphus</i>	<i>B. attica</i>	<i>H. duvernoyi</i>	<i>P. paimiri</i>	<i>P. macedoniae</i>	<i>P. major</i>	<i>S. neumayri</i>	<i>P. rouenii</i>	cf. <i>P. coelophrys</i>	<i>S. boissieri</i>
<i>Cervus elaphus</i>	Asfc epLsar													
<i>Giraffa</i> sp.	HAsfc	HAsfc epLsar												
<i>Okapia johnstoni</i>	Asfc epLsar		HAsfc epLsar											
<i>Alcelaphus buselaphus</i>	Asfc epLsar	HAsfc Asfc epLsar	Asfc epLsar	HAsfc Asfc epLsar										
<i>Bohlinia attica</i>	Asfc	epLsar	HAsfc		epLsar									
<i>Helladotherium duvernoyi</i>	HAsfc Asfc	HAsfc epLsar		HAsfc	Asfc epLsar	HAsfc								
<i>Palaeogiraffa paimiri</i>	Asfc	epLsar		epLsar	epLsar									
<i>Palaeogiraffa macedoniae</i>	epLsar	HAsfc	epLsar		Asfc	Asfc epLsar	epLsar	epLsar						
<i>Palaeogiraffa major</i>			epLsar			epLsar		epLsar						
<i>Samotherium neumayri</i>	HAsfc Asfc	HAsfc		HAsfc	epLsar	HAsfc			Asfc					
<i>Palaeotragus rouenii</i>	HAsfc Asfc	HAsfc	epLsar	HAsfc	Asfc epLsar	HAsfc		epLsar						
cf. <i>Palaeotragus coelophrys</i>	Asfc				epLsar									
<i>Samotherium boissieri</i>	epLsar		epLsar			epLsar	epLsar	epLsar						
<i>Samotherium major</i>	HAsfc	HAsfc	epLsar	HAsfc	Asfc epLsar	Asfc		epLsar			Asfc			

645 Variables were rank-transformed before analysis. When both LSD and HSD detect significant differences, the
 646 variable is underlined and in bold.

647

648 Table 4. Body anatomical traits of modern and extinct giraffids.

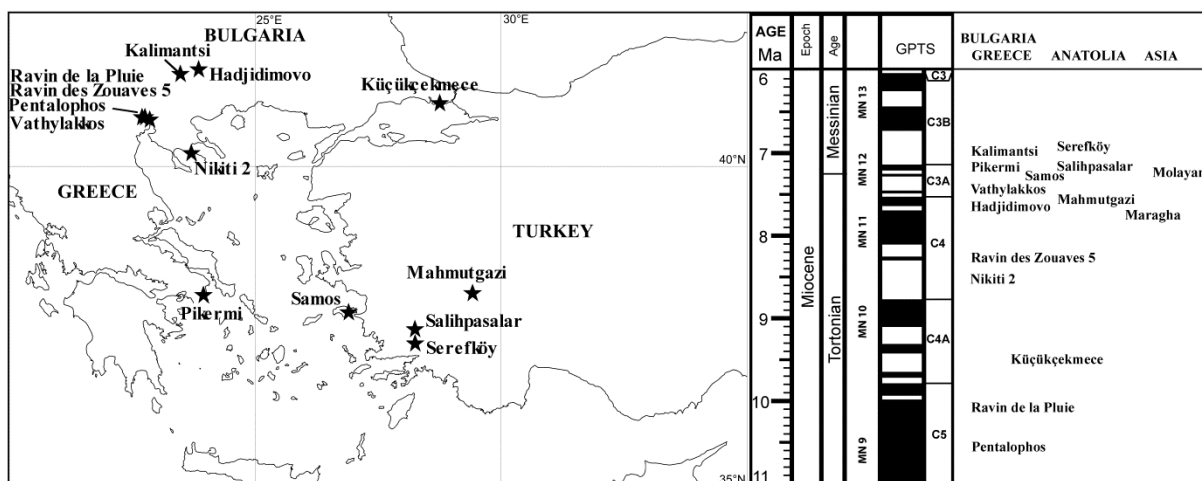
Species	Metacarpal length		Body mass estimate			Pm/M index (upper teeth)	Pm/M index (lower teeth)
	N	L	N	Humerus W	body mass		
<i>Giraffa</i> sp.	33	701	26	116	1362	75 (mean)	68 (mean)
<i>Okapia johnstoni</i>	2	307	2	75	441	74, 75	60, 65, 70
<i>Bohlinia attica</i>	6	704	7	107	1118	73, 76, 78	-
<i>Helladotherium duvernoyi</i>	20	435	15	141	2201	77, 79, 81	63, 65, 67 ⁽³⁾
<i>Palaeogiraffa macedoniae</i>	1	465	2	115	1324	72, 73, 75	65
<i>Palaeogiraffa pamiri</i>	4	469	1	115	1324	76 ?	68
<i>Palaeotragus coelophrys</i>	4	370	-	-	-	70, 71, 73, 74	68
<i>Palaeotragus rouenii</i>	5	409	6 ⁽²⁾	75	439	70, 74	63, 67, 68
<i>Samotherium boissieri</i>	14 ⁽²⁾	357	4 ⁽²⁾	104	1022	67.5 (mean of 7) ⁽¹⁾	57, 59, 60, 60
<i>Samotherium major</i>	32 ⁽²⁾	417	7 ⁽²⁾	141	2185	65, 67, 68 ⁽⁴⁾	63, 66
<i>Samotherium neumayri</i>	11	382	4	116	1341	65	58, 67

649 Metacarpal length (in mm), body mass (in kg) based upon humerus distal articular width (in mm) following the
650 equation of Scott (1990) for Ruminants (body mass = $10^{(2.5518 \cdot \log(\text{Humerus W}) + 0.4093)}$), indexes of upper and lower
651 premolar/molar rows of modern and extinct giraffids. Most data are our own, with a few additions from Bohlin
652 (1926⁽¹⁾), Kostopoulos (2009⁽²⁾, 2016⁽³⁾) and Senyürek (1954⁽⁴⁾).

653

654

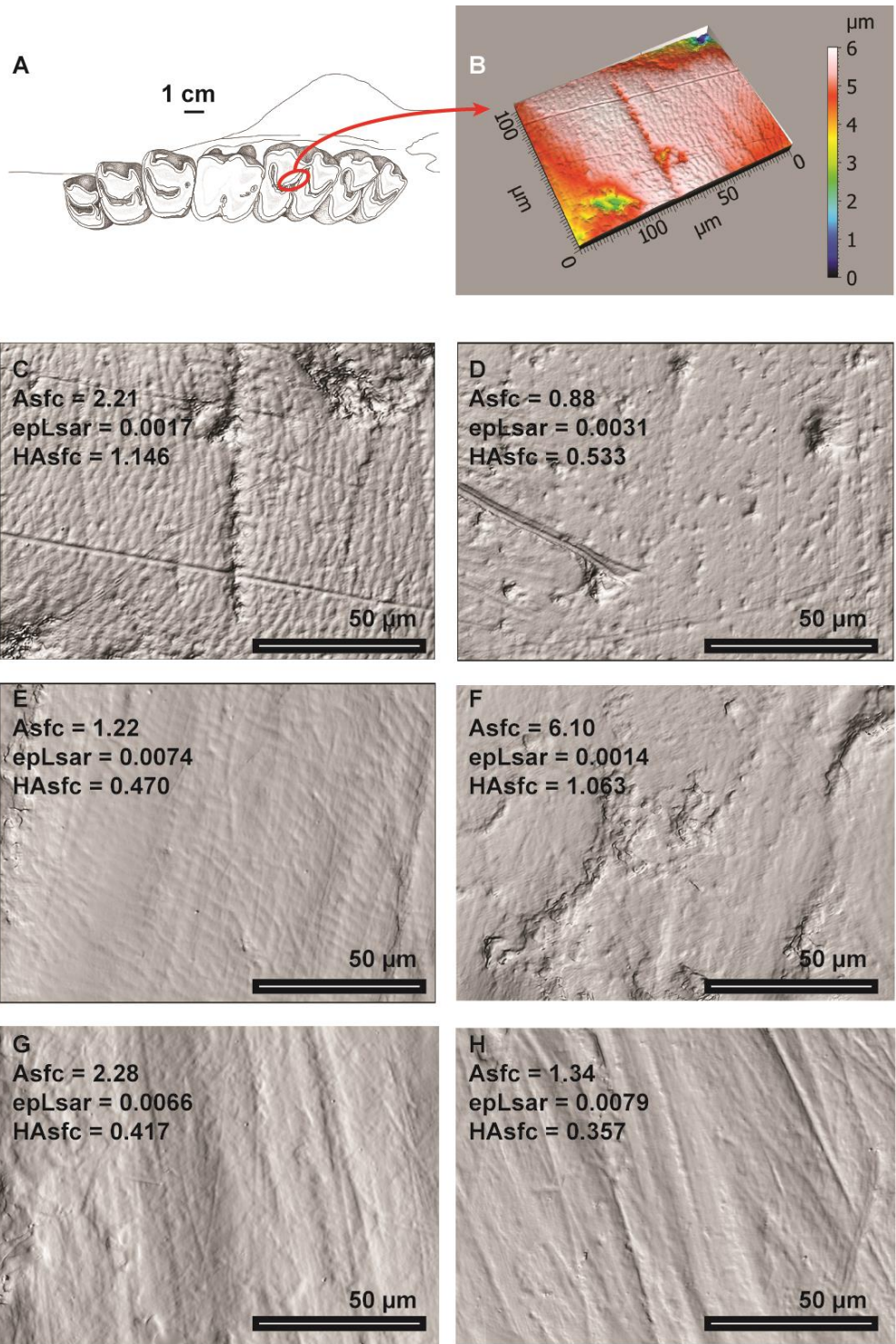
655 **Figure captions**



656

657 **Figure 1.** Geographic and chronostratigraphic distribution of the main localities considered in
 658 this study. A few specimens come from Asian (Maragha in Iran and Molayan in Afghanistan)
 659 and North African (Douaria in Tunisia) localities outside the map.

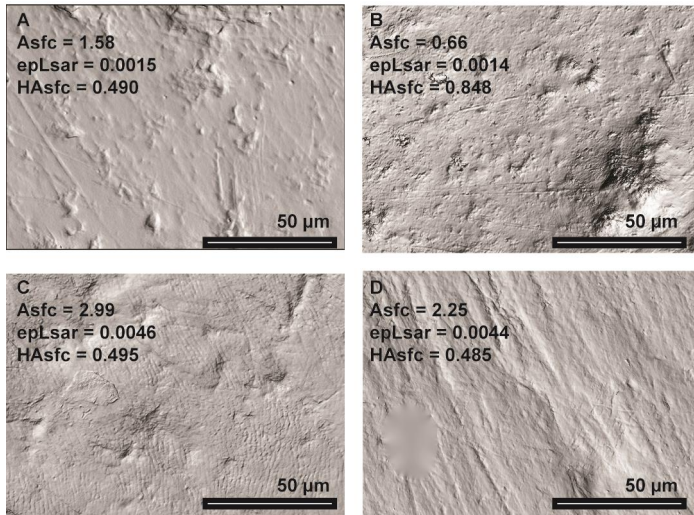
660



661

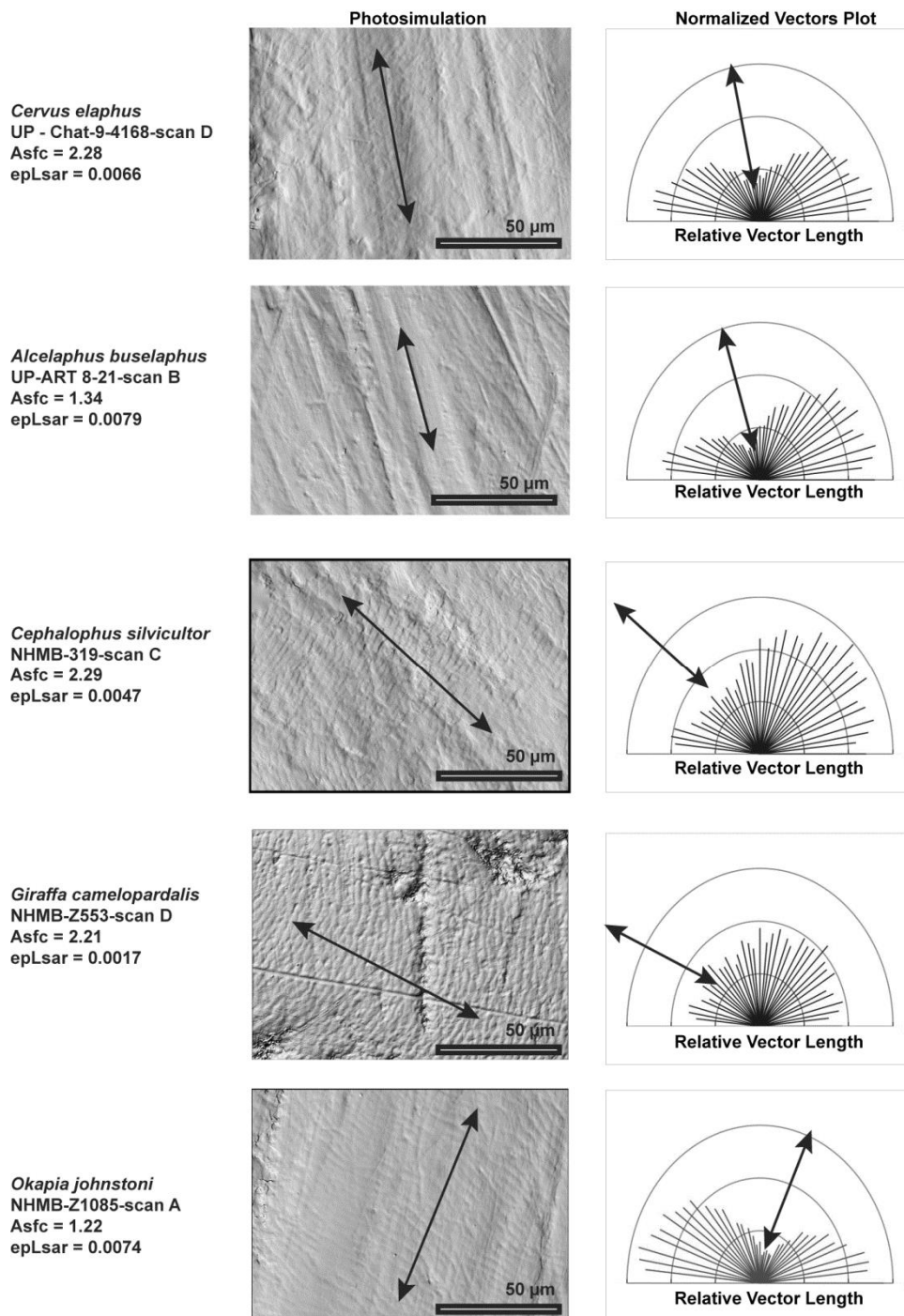
662 **Figure 2.** Occlusal view of left upper molar of a modern giraffe, *Giraffa* sp. (A; UP-M10-5-
 663 001-A) and 3D surface simulation on shearing dental facet (B; NHMB-Z553). The
 664 photomicrographs C-H were generated through the LeicaMap 7.0: *Giraffa* sp. (C: NHMB-
 665 Z553), *Okapia johnstoni* (D: NHMB-Z245; E: NHMB-Z1085), *Cephalophus silvicultor* (F:
 666 NHMB-1611), *Cervus elaphus* (G: UP-Chat-9-4168) and *Alcelaphus buselaphus* (H: UP-
 667 ART8-21).

668



669

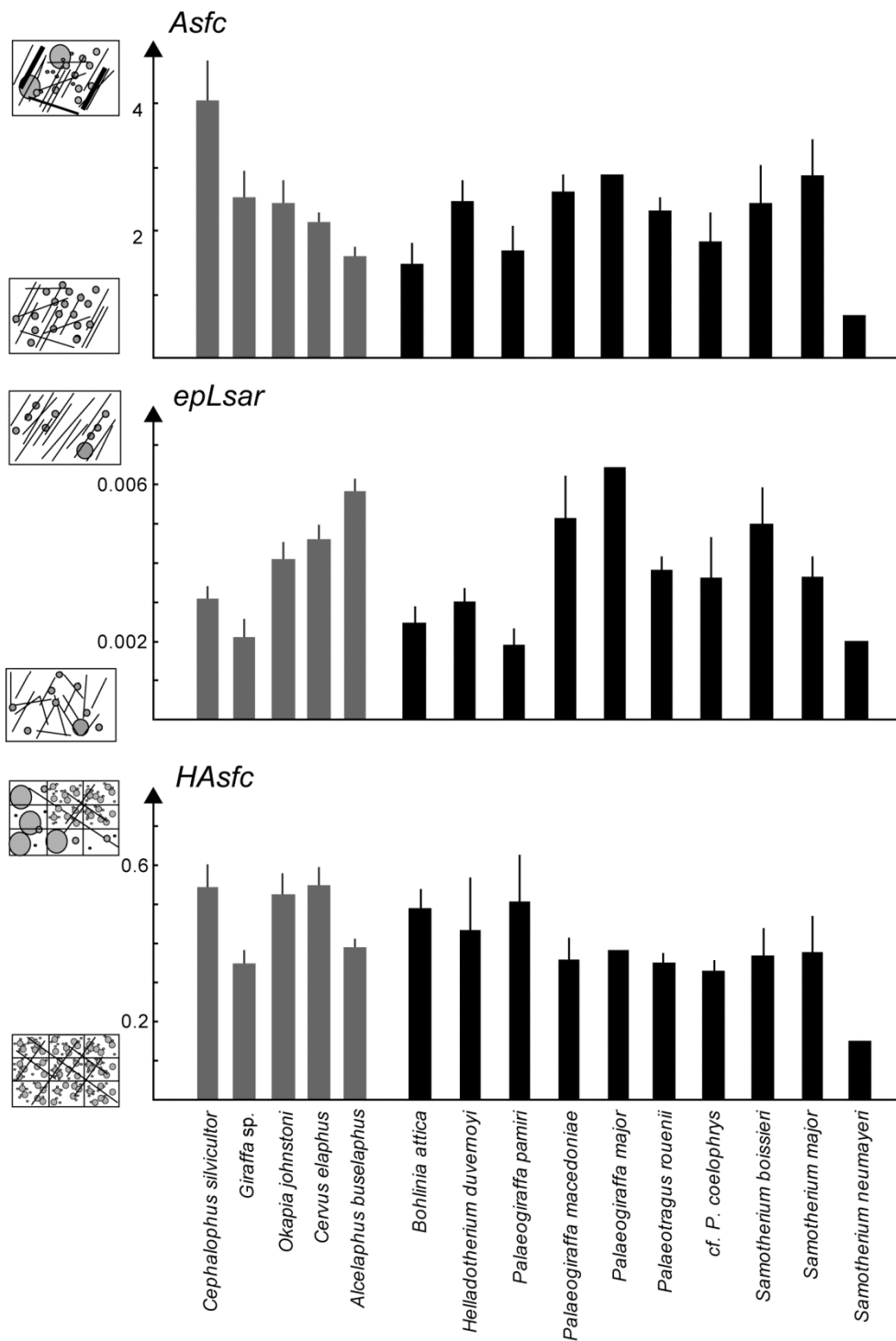
670 **Figure 3.** The photosimulations A-D were generated through the LeicaMap 7.4:
671 *Helladotherium duvernoyi* from Kalimansti, Bulgaria (A; K5159), *Palaeogiraffa pamiri* from
672 Küçükçekmeçe, Turkey (B; MNHN-TRQ-430), *Palaeotragus rouenii* from Pikermi, Greece
673 (C; MNHN-PIK-1672), and *Samotherium major* from Salihpasalar, Turkey (D; MTA-MYS-
674 843).
675



676

677 **Figure 4.** Photosimulations of dental microwear textures of modern ruminants with values in
 678 complexity (Asfc) and anisotropy (epLsar) and the corresponding rosette plot of relative
 679 lengths taken at 36 different orientations. The two first surfaces (*Cervus elaphus* and
 680 *Alcelaphus buselaphus*) display low relative length correlated with the main microwear
 681 textural orientation (here the main directionality is highlighted with the black arrows). The
 682 last three surfaces (*Cephalophus silvicultor*, *Giraffa camelopardalis* and *Okapia johnstoni*)
 683 display a main orientation of dental microwear textures disconnected from the perikemata
 684 direction, meaning that anisotropy does not reflect the perikemata directionality, but the
 685 dental microwear texture one.

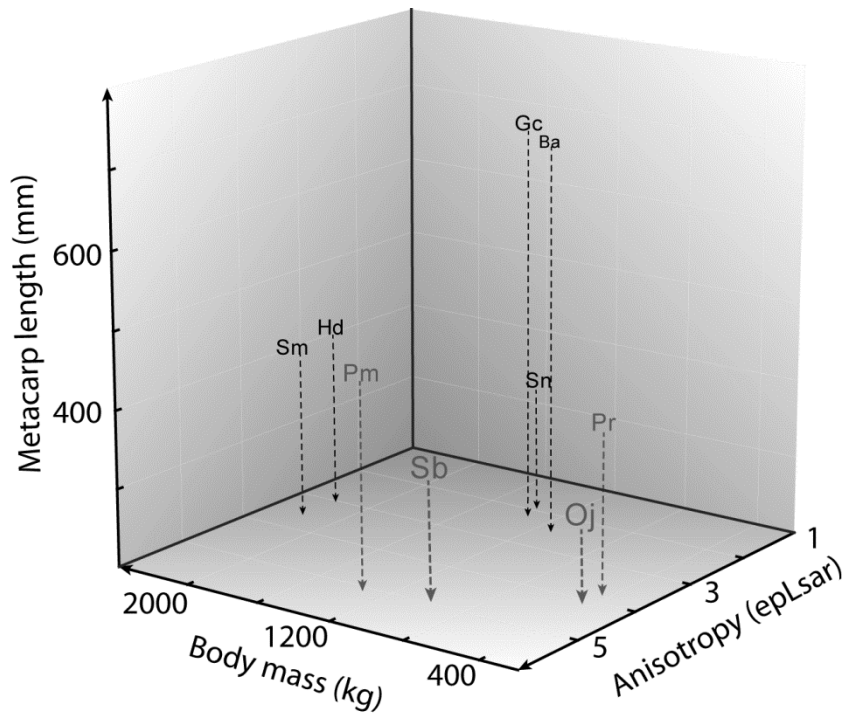
686



687

688 **Figure 5.** Bar plots (mean and standard error of the mean) of dental microwear textural
 689 parameters Asfc: complexity; epLsar: anisotropy calculated at the 1.8 μm scale; HAsfc:
 690 Heterogeneity of complexity (calculated with a 9-cell mesh) for modern ruminants (in gray)
 691 and extinct giraffids (in black).

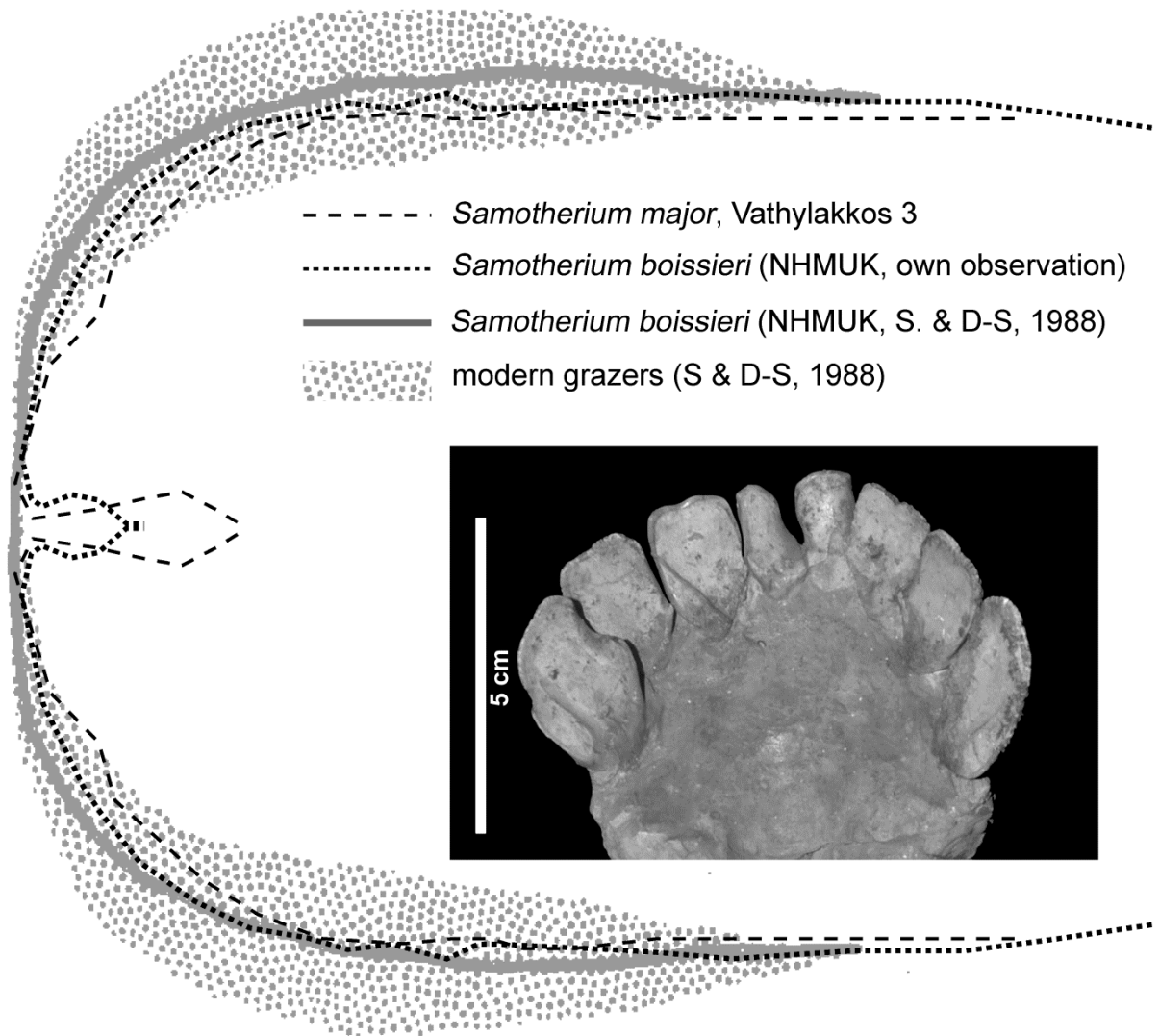
692



693

694 **Figure 6.** 3D plot of the average of anisotropy (epLsar) of the dental microwear textures vs.
 695 averages of body mass (in kg) and length of metacarpal bone (in mm), which approximates
 696 the height at the withers. Note that specimens used for body traits and dental microwear
 697 analysis are not the same (see Table 4).

698



699

700 **Figure 7.** Outlines of the premaxilla in *Samotherium*. Square outline denotes grazers. S & D-
 701 S: Solounias and Dawson-Saunders (1988); outline of *S. major* based upon the specimen from
 702 Vathylakkos 3 (Geraads, 1978); outlines of *S. boissieri* based upon NHMUK M4215.

703

704

705 Appendix 1 - List of extant and extinct specimens with surface parameters

State	Species	Individual	Asfc	epLsar 1.8 µm	Hasfc 9 cells
Extant species	Alcelaphus buselaphus	MNHN-1894-1524	1.56	0.00480	0.381
Extant species	Alcelaphus buselaphus	MNHN-1913-39	0.52	0.00166	0.491
Extant species	Alcelaphus buselaphus	MNHN-1913-744	0.87	0.00339	0.297
Extant species	Alcelaphus buselaphus	MNHN-1965-1099	1.52	0.00736	0.272
Extant species	Alcelaphus buselaphus	MNHN-1965-1101	0.73	0.00398	0.405
Extant species	Alcelaphus buselaphus	MNHN-1965-1104	1.16	0.00545	0.519
Extant species	Alcelaphus buselaphus	MNHN-1965-1105	1.02	0.00491	0.199
Extant species	Alcelaphus buselaphus	MNHN-1965-1107	1.08	0.00525	0.270
Extant species	Alcelaphus buselaphus	MNHN-1970-31	1.97	0.00709	0.366
Extant species	Alcelaphus buselaphus	MNHN-1970-34	1.94	0.00740	0.312
Extant species	Alcelaphus buselaphus	MNHN-1970-35	1.76	0.00517	0.424
Extant species	Alcelaphus buselaphus	MNHN-1974-211	1.19	0.00564	0.329
Extant species	Alcelaphus buselaphus	MNHN-BUB-6	0.87	0.00360	0.249
Extant species	Alcelaphus buselaphus	MNHN-BUB-8	2.40	0.00417	0.446
Extant species	Alcelaphus buselaphus	SMNK-1027	1.14	0.00507	0.302
Extant species	Alcelaphus buselaphus	SMNK-1206	1.29	0.00680	0.791
Extant species	Alcelaphus buselaphus	SMNK-1207	1.18	0.00796	0.333
Extant species	Alcelaphus buselaphus	SMNK-126	0.94	0.00706	0.339
Extant species	Alcelaphus buselaphus	SMNK-2358	2.40	0.00759	0.401
Extant species	Alcelaphus buselaphus	SMNK-47	1.72	0.00673	0.345
Extant species	Alcelaphus buselaphus	UP-ART-8-22	3.53	0.00622	0.344
Extant species	Alcelaphus buselaphus	UP-ART-8-26	2.57	0.00529	0.608
Extant species	Alcelaphus buselaphus	UP-ART-8-27	3.69	0.00555	0.561
Extant species	Alcelaphus buselaphus	UP-ART-8-20	1.48	0.00610	0.400
Extant species	Alcelaphus buselaphus	UP-ART-8-21	1.34	0.00796	0.357
Extant species	Alcelaphus buselaphus	UP-ART-8-23	1.24	0.00650	0.358
Extant species	Alcelaphus buselaphus	UP-ART-8-24	2.05	0.00913	0.399
Extant species	Alcelaphus buselaphus	UP-ART-8-25	1.71	0.00466	0.361
Extant species	Cephalophus silivicultor	NHMB-Csilv-14	8.18	0.00175	0.504
Extant species	Cephalophus silivicultor	NHMB-Csilv-1611	2.96	0.00607	0.289
Extant species	Cephalophus silivicultor	NHMB-Csilv-1612	2.65	0.00101	0.520
Extant species	Cephalophus silivicultor	NHMB-Csilv-1616	2.11	0.00290	0.497
Extant species	Cephalophus silivicultor	NHMB-Csilv-1617	3.51	0.00428	0.467
Extant species	Cephalophus silivicultor	NHMB-Csilv-319	4.11	0.00288	1.325
Extant species	Cephalophus silivicultor	NHMB-Csilv-366	2.21	0.00615	0.384
Extant species	Cephalophus silivicultor	NHMB-Csilv-578	3.32	0.00256	0.813
Extant species	Cephalophus silivicultor	NHMB-Csilv-878	6.06	0.00139	1.089
Extant species	Cephalophus silivicultor	NHMB-Csilv-924	2.07	0.00426	0.317
Extant species	Cephalophus silivicultor	NHMB-Csilv-DIE-1	17.03	0.00063	0.605
Extant species	Cephalophus silivicultor	NHMB-Csilv-GM4	3.06	0.00211	0.975
Extant species	Cephalophus silivicultor	NHMB-Csilv-R12923	1.45	0.00223	0.156
Extant species	Cephalophus silivicultor	NHMB-Csilv-R16753	2.66	0.00191	0.427
Extant species	Cephalophus silivicultor	NHMB-Csilv-SN-DIB-95	1.52	0.00454	0.318
Extant species	Cephalophus silivicultor	NHMB-Csilv-Z2039-2	2.62	0.00209	0.280
Extant species	Cephalophus silivicultor	NHMB-Csilv-Z3048	7.53	0.00153	0.283
Extant species	Cephalophus silivicultor	NHMB-Csilv-Z3344	2.15	0.00460	0.359
Extant species	Cephalophus silivicultor	NHMB-Csilv-Z3347	3.43	0.00460	0.623
Extant species	Cephalophus silivicultor	NHMB-Csilv-Z352	1.95	0.00476	0.338
Extant species	Cephalophus silivicultor	NHMB-Csilv-Z3669	2.11	0.00312	0.334
Extant species	Cephalophus silivicultor	NHMB-Csilv-Z3916	5.29	0.00355	0.749
Extant species	Cephalophus silivicultor	NHMB-Csilv-Z3918	3.53	0.00476	0.344
Extant species	Cephalophus silivicultor	NHMB-Csilv-Z404	6.10	0.00140	1.063
Extant species	Cephalophus silivicultor	NHMB-Csilv-Z464	3.07	0.00170	0.455

706

707

State	Species	Individual	Asfc	epLsar 1.8 µm	Hasfc 9 cells
Extant species	Cervus elaphus	UP-Chat9-1023	1.65	0.00263	1.127
Extant species	Cervus elaphus	UP-Chat9-1024	1.02	0.00388	0.594
Extant species	Cervus elaphus	UP-Chat9-1025	1.54	0.00400	1.229
Extant species	Cervus elaphus	UP-Chat9-1035	2.72	0.00063	1.055
Extant species	Cervus elaphus	UP-Chat9-1037	3.17	0.00491	0.595
Extant species	Cervus elaphus	UP-Chat9-1038	1.98	0.00646	0.311
Extant species	Cervus elaphus	UP-Chat9-1039	1.71	0.00835	0.584
Extant species	Cervus elaphus	UP-Chat9-2054	2.92	0.00531	0.527
Extant species	Cervus elaphus	UP-Chat9-2057	3.17	0.00523	0.742
Extant species	Cervus elaphus	UP-Chat9-3105	1.18	0.00457	0.516
Extant species	Cervus elaphus	UP-Chat9-3132	2.69	0.00057	0.380
Extant species	Cervus elaphus	UP-Chat9-3133	1.65	0.00391	0.486
Extant species	Cervus elaphus	UP-Chat9-4152	1.14	0.00451	0.451
Extant species	Cervus elaphus	UP-Chat9-4157	0.95	0.00596	0.199
Extant species	Cervus elaphus	UP-Chat9-4159	1.57	0.00567	0.196
Extant species	Cervus elaphus	UP-Chat9-4161	1.70	0.00373	0.510
Extant species	Cervus elaphus	UP-Chat9-4167	2.49	0.00715	0.457
Extant species	Cervus elaphus	UP-Chat9-4168	2.28	0.00655	0.417
Extant species	Cervus elaphus	UP-Chat9-4180	1.80	0.00411	0.290
Extant species	Cervus elaphus	UP-Chat9-4189	2.79	0.00557	0.578
Extant species	Cervus elaphus	UP-Chat9-4190	1.42	0.00511	0.467
Extant species	Cervus elaphus	UP-Chat9-4264	2.87	0.00169	0.824
Extant species	Cervus elaphus	UP-Chat9-4271	1.86	0.00402	0.486
Extant species	Cervus elaphus	UP-Chat9-4278	1.57	0.00688	0.589
Extant species	Cervus elaphus	UP-Chat9-4295	1.45	0.00153	0.320
Extant species	Cervus elaphus	UP-Chat9-4302	3.69	0.00291	0.477
Extant species	Cervus elaphus	UP-Chat9-4319	3.96	0.00547	0.551
Extant species	Cervus elaphus	UP-Chat9-4339	2.06	0.00654	0.602
Extant species	Cervus elaphus	UP-Chat9-4354	2.43	0.00518	0.283
Extant species	Giraffa sp.	KNM-no#-Z7	1.43	0.00234	0.241
Extant species	Giraffa sp.	KNM-OM-2087	1.31	0.00190	0.401
Extant species	Giraffa sp.	KNM-OM-2275	2.70	0.00141	0.190
Extant species	Giraffa sp.	MNHN-1928-307	2.90	0.00179	0.446
Extant species	Giraffa sp.	NHMB-Z-1086	1.46	0.00613	0.254
Extant species	Giraffa sp.	NHMB-Z-553	2.21	0.00171	0.300
Extant species	Giraffa sp.	SMNS-30171	3.06	0.00192	0.481
Extant species	Giraffa sp.	SNG-35595	1.82	0.00066	0.311
Extant species	Giraffa sp.	SNG-36628	1.76	0.00126	0.298
Extant species	Giraffa sp.	SNG-497	2.98	0.00043	0.350
Extant species	Giraffa sp.	SNG-498	1.76	0.00415	0.279
Extant species	Giraffa sp.	SNG-501	6.75	0.00149	0.606
Extant species	Okapia johnstoni	MRAC-1025	3.10	0.00226	0.474
Extant species	Okapia johnstoni	MRAC-1192	3.93	0.00461	0.381
Extant species	Okapia johnstoni	MRAC-1193	4.48	0.00174	0.371
Extant species	Okapia johnstoni	MRAC-2904	1.38	0.00608	0.433
Extant species	Okapia johnstoni	MRAC-3074	3.19	0.00427	0.483
Extant species	Okapia johnstoni	MRAC-3075	2.82	0.00151	0.375
Extant species	Okapia johnstoni	MRAC-3076	2.37	0.00454	0.260
Extant species	Okapia johnstoni	MRAC-4051	1.32	0.00762	0.636
Extant species	Okapia johnstoni	MRAC-6293	1.99	0.00246	1.302
Extant species	Okapia johnstoni	MRAC-705B	4.49	0.00061	0.442
Extant species	Okapia johnstoni	MRAC-8358	1.82	0.00542	0.445
Extant species	Okapia johnstoni	MRAC-8663	3.36	0.00127	0.552
Extant species	Okapia johnstoni	MRAC-9726	2.23	0.00634	0.230
Extant species	Okapia johnstoni	MRAC-9727	1.81	0.00537	0.774
Extant species	Okapia johnstoni	NHMB-Z-1085	1.22	0.00738	0.470
Extant species	Okapia johnstoni	NHMB-Z-243	1.69	0.00346	0.603
Extant species	Okapia johnstoni	NHMB-Z-245	0.88	0.00311	0.533
Extant species	Okapia johnstoni	NHMB-Z-2908	0.74	0.00472	0.208
Extant species	Okapia johnstoni	NHMB-Z-329	2.36	0.00268	1.019
Extant species	Okapia johnstoni	NHMB-Z-576	4.42	0.00288	0.133
Extant species	Okapia johnstoni	NMHB-C3899	0.44	0.00192	0.603
Extant species	Okapia johnstoni	NMHB-C3900	0.56	0.00279	0.533
Extant species	Okapia johnstoni	NHMB-Z-2308	1.32	0.00749	0.276
Extant species	Okapia johnstoni	NHMB-Z-244	6.27	0.00544	0.534
Extant species	Okapia johnstoni	NHMB-Z-3686	3.26	0.00585	0.887

State	Species	Individual	Asfc	eP ₁ sar 1.8 µm	Hasfc 9 cells	Region	Site
Extinct species	<i>Bohlinia attica</i>	LGPU-T-NKT-147-UM2	0.91	0.00211	0.343	Greece	Nikiti-1
Extinct species	<i>Bohlinia attica</i>	AM-NMNHS-K 5206	1.07	0.00317	0.533	Bulgaria	Kalimantsi
Extinct species	<i>Bohlinia attica</i>	AM-NMNHS-K 5209	1.23	0.00301	0.518	Bulgaria	Kalimantsi
Extinct species	<i>Bohlinia attica</i>	LGPU-T-NKT-148-UM2	1.44	0.00097	0.432	Greece	Nikiti-1
Extinct species	<i>Bohlinia attica</i>	LGPU-T-NKT-145-UM2	2.72	0.00307	0.618	Greece	Nikiti-1
Extinct species	<i>Palaeogiraffa paimiri</i>	MNHN TRQ-430	0.66	0.00142	0.259	Turkey	Küçükçekmece
Extinct species	<i>Palaeogiraffa paimiri</i>	MNHN TRQ-428	0.78	0.00215	0.433	Turkey	Küçükçekmece
Extinct species	<i>Palaeogiraffa paimiri</i>	MNHN TRQ-424	1.10	0.00103	0.317	Turkey	Küçükçekmece
Extinct species	<i>Palaeogiraffa paimiri</i>	MNHN TRQ-422	2.36	0.00131	0.533	Turkey	Küçükçekmece
Extinct species	<i>Palaeogiraffa paimiri</i>	MNHN TRQ-425	2.56	0.00187	0.427	Turkey	Küçükçekmece
Extinct species	<i>Palaeogiraffa paimiri</i>	MNHN TRQ-432	2.62	0.00372	1.068	Turkey	Küçükçekmece
Extinct species	<i>Helladotherium duvernoyi</i>	AM-NMNHS-HD 5157	0.88	0.00343	0.645	Bulgaria	Hadjidimovo
Extinct species	<i>Helladotherium duvernoyi</i>	AM-NMNHS-K 5198	1.06	0.00290	0.207	Bulgaria	Kalimantsi
Extinct species	<i>Helladotherium duvernoyi</i>	MNHN-PIK1501	1.08	0.00278	0.267	Greece	Pikermi
Extinct species	<i>Helladotherium duvernoyi</i>	AM-NMNHS-K 5159	1.58	0.00146	0.490	Bulgaria	Kalimantsi
Extinct species	<i>Helladotherium duvernoyi</i>	AM-NMNHS-HD 5200	1.69	0.00471	0.747	Bulgaria	Hadjidimovo
Extinct species	<i>Helladotherium duvernoyi</i>	FSL16753-M1	2.12	0.00137	0.249	Algeria	Douaria
Extinct species	<i>Helladotherium duvernoyi</i>	AM-NMNHS-K 5161	2.23	0.00187	0.106	Bulgaria	Kalimantsi
Extinct species	<i>Helladotherium duvernoyi</i>	LGPU-T-NIK 1804	2.27	0.00555	0.298	Greece	Nikiti-2
Extinct species	<i>Helladotherium duvernoyi</i>	LGPU-T-NIK 1057	2.32	0.00472	0.250	Greece	Nikiti-2
Extinct species	<i>Helladotherium duvernoyi</i>	LGPU-T-NIK 1	2.34	0.00362	0.152	Greece	Nikiti-2
Extinct species	<i>Helladotherium duvernoyi</i>	AM-NMNHS-K 5156	2.50	0.00138	0.221	Bulgaria	Kalimantsi
Extinct species	<i>Helladotherium duvernoyi</i>	LGPU-T-RZO189	3.52	0.00128	0.177	Greece	Ravin des Zouaves-5
Extinct species	<i>Helladotherium duvernoyi</i>	AM-NMNHS-HD 5204	4.01	0.00292	0.239	Bulgaria	Hadjidimovo
Extinct species	<i>Helladotherium duvernoyi</i>	AM-NMNHS-K 5197	4.55	0.00421	2.179	Bulgaria	Kalimantsi
Extinct species	<i>Helladotherium duvernoyi</i>	MNHN-MNHN-PIK1500	4.77	0.00280	0.264	Greece	Pikermi
Extinct species	<i>Palaeogiraffa macedoniae</i>	LGPU-T-PNT 137	2.00	0.00150	0.329	Greece	Pentalophos
Extinct species	<i>Palaeogiraffa macedoniae</i>	LGPU-T-PNT 328	2.01	0.00682	0.357	Greece	Pentalophos
Extinct species	<i>Palaeogiraffa macedoniae</i>	LGPU-T-PNT 136	2.33	0.00669	0.194	Greece	Pentalophos
Extinct species	<i>Palaeogiraffa macedoniae</i>	LGPU-T-PNT 112	2.75	0.00346	0.488	Greece	Pentalophos
Extinct species	<i>Palaeogiraffa macedoniae</i>	LGPU-T-PNT 111A	2.86	0.00376	0.220	Greece	Pentalophos
Extinct species	<i>Palaeogiraffa macedoniae</i>	LGPU-T-PNT 121	3.72	0.00851	0.545	Greece	Pentalophos
Extinct species	<i>Palaeogiraffa major</i>	LGPU-T-RPL 734	2.87	0.00641	0.381	Greece	Ravin de la Pluie
Extinct species	<i>P. coelophrys</i>	MNHN-MAR-669	1.30	0.00108	0.419	Iran	Maragheh
Extinct species	<i>P. coelophrys</i>	LGPU-T-RPL104	1.32	0.00592	0.304	Greece	Ravin de la Pluie
Extinct species	<i>P. coelophrys</i>	LGPU-T-PNT113	2.91	0.00379	0.287	Greece	Pentalophos
Extinct species	<i>Palaeotragerus rouenii</i>	MNHN-MOL-4211	0.68	0.00400	0.341	Afghanistan	Molayan
Extinct species	<i>Palaeotragerus rouenii</i>	MNHN-MOL-4201	0.78	0.00488	0.363	Afghanistan	Molayan
Extinct species	<i>Palaeotragerus rouenii</i>	LGPU-T-DIT-2-UM2-a.sur	1.15	0.00554	0.175	Greece	Dytiko
Extinct species	<i>Palaeotragerus rouenii</i>	NHML-PIK-M11453#5	1.39	0.00131	0.284	Greece	Pikermi
Extinct species	<i>Palaeotragerus rouenii</i>	LGPU-T-RPI-91b-UM2	1.40	0.00650	0.422	Greece	Ravin de la Pluie
Extinct species	<i>Palaeotragerus rouenii</i>	NHML-PIK-M11419#7	1.46	0.00235	0.271	Greece	Pikermi
Extinct species	<i>Palaeotragerus rouenii</i>	NHML-PIK-M11419#3	1.78	0.00338	0.429	Greece	Pikermi
Extinct species	<i>Palaeotragerus rouenii</i>	AMNHS-MTLB52	1.80	0.00483	0.232	Greece	Mytilinii B
Extinct species	<i>Palaeotragerus rouenii</i>	MTA-MYS351	1.81	0.00573	0.299	Turkey	Serefköy-2
Extinct species	<i>Palaeotragerus rouenii</i>	MNHN-MOL-4212	1.93	0.00266	0.732	Afghanistan	Molayan
Extinct species	<i>Palaeotragerus rouenii</i>	LGPU-T-DIT-3-UM2	2.04	0.00342	0.221	Greece	Dytiko
Extinct species	<i>Palaeotragerus rouenii</i>	MNHN-PIK1671	2.19	0.00277	0.371	Greece	Pikermi
Extinct species	<i>Palaeotragerus rouenii</i>	AM-NMNHS-HD 5190	2.43	0.00228	0.372	Bulgaria	Hadjidimovo
Extinct species	<i>Palaeotragerus rouenii</i>	NHMEU-PV-1598	2.58	0.00493	0.299	Turkey	Serefköy-2
Extinct species	<i>Palaeotragerus rouenii</i>	NHMEU-PV-1629	2.69	0.00610	0.348	Turkey	Serefköy-2
Extinct species	<i>Palaeotragerus rouenii</i>	MNHN-PIK1672	2.99	0.00464	0.388	Greece	Pikermi
Extinct species	<i>Palaeotragerus rouenii</i>	AMNHS-MTLB128	3.53	0.00457	0.378	Greece	Mytilinii B
Extinct species	<i>Palaeotragerus rouenii</i>	NHML-PIK M11419#9	3.66	0.00493	0.298	Greece	Pikermi
Extinct species	<i>Palaeotragerus rouenii</i>	MTA-MYS-299	3.75	0.00144	0.457	Turkey	Serefköy-1
Extinct species	<i>Palaeotragerus rouenii</i>	MNHN-PIK1674	3.77	0.00225	0.366	Greece	Pikermi
Extinct species	<i>Palaeotragerus rouenii</i>	NHML-PIKM11419#4	4.40	0.00129	0.282	Greece	Pikermi
Extinct species	<i>Samotherium boissieri</i>	NHMB-Sam29	0.76	0.00651	0.408	Greece	Samos
Extinct species	<i>Samotherium boissieri</i>	NHML-Samos-M-4226	1.39	0.00658	0.179	Greece	Samos
Extinct species	<i>Samotherium boissieri</i>	NHML-Samos-M-4235	2.67	0.00418	0.418	Greece	Samos
Extinct species	<i>Samotherium boissieri</i>	NHML-Samos-M4234d-No14	3.41	0.00163	0.559	Greece	Samos
Extinct species	<i>Samotherium boissieri</i>	NHML-Samos-M-4241	3.93	0.00596	0.302	Greece	Samos
Extinct species	<i>Samotherium major</i>	LGPU-T-VAT-157-Im2	1.41	0.00481	0.178	Greece	Vathylakkos
Extinct species	<i>Samotherium major</i>	AMNHS-MTLA-540	1.59	0.00530	0.429	Greece	Mytilinii A
Extinct species	<i>Samotherium major</i>	AMNHS-MTLA-311	1.79	0.00545	0.228	Greece	Mytilinii A
Extinct species	<i>Samotherium major</i>	MTA-MYS-843	2.25	0.00441	0.279	Turkey	Salihpasalar
Extinct species	<i>Samotherium major</i>	AMNHS-MTLB95	2.71	0.00479	0.336	Greece	Mytilinii B
Extinct species	<i>Samotherium major</i>	MTA-MYS-848	4.63	0.00089	0.562	Turkey	Salihpasalar
Extinct species	<i>Samotherium major</i>	MTA-MYS-620	4.95	0.00238	0.939	Turkey	Serefköy-1
Extinct species	<i>Samotherium major</i>	MTA-MYS-847	5.21	0.00198	0.159	Turkey	Salihpasalar
Extinct species	<i>Samotherium major</i>	SMNK-MA3	1.16	0.00325	0.254	Turkey	Mahmut Ghazi
Extinct species	<i>Samotherium neumayeri</i>	MNHN-MAR-528	0.66	0.00199	0.149	Iran	Maragheh